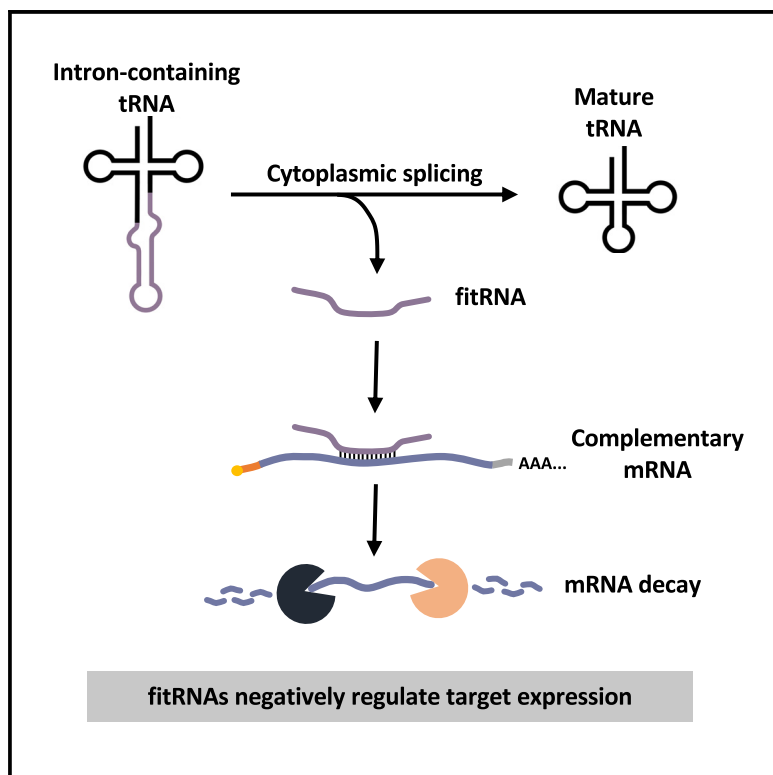


Free introns of tRNAs as complementarity-dependent regulators of gene expression

Graphical abstract



Authors

Regina T. Nostramo, Paolo L. Sinopoli,
Alicia Bao, Sara Metcalf,
Lauren M. Peltier, Anita K. Hopper

Correspondence

hopper.64@osu.edu

In brief

Nostramo et al. demonstrate that free introns of tRNAs (fitRNAs) are a previously unknown class of small noncoding regulatory RNAs that bind to complementary sequences on mRNA ORFs, leading to decay. fitRNAs accumulate under certain stresses and thereby regulate mRNA levels under basal and stress conditions.

Highlights

- tRNA introns possess remarkable complementarity to ORFs in *S. cerevisiae*
- tRNA introns base pair with complementary mRNA sequences, resulting in mRNA decay
- Oxidative stress increases free tRNA^{Trp} intron and decreases complementary mRNAs
- Free introns of tRNAs (fitRNAs) are a previously unknown class of small regulatory RNAs



Article

Free introns of tRNAs as complementarity-dependent regulators of gene expression

Regina T. Nostramo,¹ Paolo L. Sinopoli,¹ Alicia Bao,^{1,3} Sara Metcalf,¹ Lauren M. Peltier,^{1,4} and Anita K. Hopper^{1,2,5,*}

¹Department of Molecular Genetics & Center for RNA Biology, The Ohio State University, Columbus, OH 43210, USA

²Comprehensive Cancer Center Ohio State University, Columbus, OH 43210, USA

³Present address: Thomas Jefferson University Hospital, Philadelphia, PA 19107, USA

⁴Present address: The University of Toledo, College of Medicine and Life Sciences, Toledo, OH 43606, USA

⁵Lead contact

*Correspondence: hopper.64@osu.edu

<https://doi.org/10.1016/j.molcel.2025.01.019>

SUMMARY

From archaea to humans, a subset of transfer RNA (tRNA) genes possesses an intron that must be removed from transcribed pre-tRNAs to generate mature, functional tRNAs. Evolutionary conservation of tRNA intron sequences suggests that tRNA introns perform sequence-dependent cellular functions, which are presently unknown. Here, we demonstrate that free introns of tRNAs (fitRNAs) in *Saccharomyces cerevisiae* serve as small regulatory RNAs that inhibit mRNA levels via long (13–15 nt) statistically improbable stretches of (near) perfect complementarity to mRNA coding regions. The functions of fitRNAs are both constitutive and inducible because genomic deletion or inducible overexpression of tRNA^{Ile} introns led to corresponding increases or decreases in levels of complementary mRNAs. Remarkably, although tRNA introns are usually rapidly degraded, fitRNA^{Trp} selectively accumulates following oxidative stress, and target mRNA levels decrease. Thus, fitRNAs serve as gene regulators that fine-tune basal mRNA expression and alter the network of mRNAs that respond to oxidative stress.

INTRODUCTION

Transfer RNAs (tRNAs) are small noncoding RNAs (snRNAs) that function as essential adaptor molecules in protein synthesis. In addition to this canonical role, tRNAs serve other functions, such as regulating gene expression, apoptosis, the immune response, and cellular responses to stress.^{1–3} As a result, defects in tRNA biology have detrimental impacts on human health, leading to diseases such as neurological disorders and cancer.⁴ A recent resurgence in tRNA research has brought into focus the emerging complexity of tRNA biology. This includes the identification and functional characterization of numerous tRNA modifications, tRNA-interacting proteins, and tRNA fragments (tRFs).^{2,5,6} Here, we identify tRNA introns as another tier of regulatory complexity in tRNA biology.

From archaea to humans, a subset of tRNA genes contain an intron. The canonical tRNA intron is a short sequence located one nucleotide (nt) 3' to the anticodon, dividing the tRNA roughly in half into 5' and 3' exons. Although the presence of the intron does not alter the tRNA's L-shaped tertiary structure, it does change the anticodon loop structure.^{7–12} Therefore, introns must be excised to generate tRNAs that are functional in translation. Since all annotated eukaryotes possess at least one tRNA family for which all reiterated genes contain an intron,¹³ splicing of tRNA introns is essential to fully decode the genome into the proteome.

In all organisms, except eubacteria,^{14,15} tRNA splicing is mediated by the tRNA splicing endonuclease complex (TSEN in humans, SEN in yeast). The role of the TSEN/SEN complex in tRNA splicing is highly conserved,^{16,17} however its subcellular localization varies. In vertebrates, the TSEN complex is nucleoplasmic,^{16,18,19} but in plants, protozoa, and yeasts, tRNA splicing occurs in the cytoplasm after pre-tRNA nuclear export.⁵ In fact, in *Saccharomyces cerevisiae* and *Schizosaccharomyces pombe*, the SEN complex localizes to the cytoplasmic surface of mitochondria.^{20,21}

Although the primary function of tRNA splicing is to generate mature tRNAs, a byproduct of the reaction is excised tRNA intron. In yeast, this intron generally remains linear^{22,23} and contains a 5' hydroxyl group and a 2', 3' cyclic phosphate at the 3' end.^{16,17,22} However, in archaea and animals, tRNA introns can circularize.^{24,25} Even though there are approximately 600,000 free tRNA introns produced per generation in yeast, they are barely detectable under standard growth conditions due to rapid degradation.²³ One mechanism of tRNA intron turnover requires 5' end phosphorylation by the RNA kinase activity of the tRNA ligase Trl1/Rlg1, followed by 5'-3' degradation by the cytoplasmic exonuclease, Xrn1.²³ However, it is unknown whether all families of tRNA introns are degraded in this manner.

The presence of introns in tRNA genes is evolutionarily conserved; however, there is wide variability in the properties



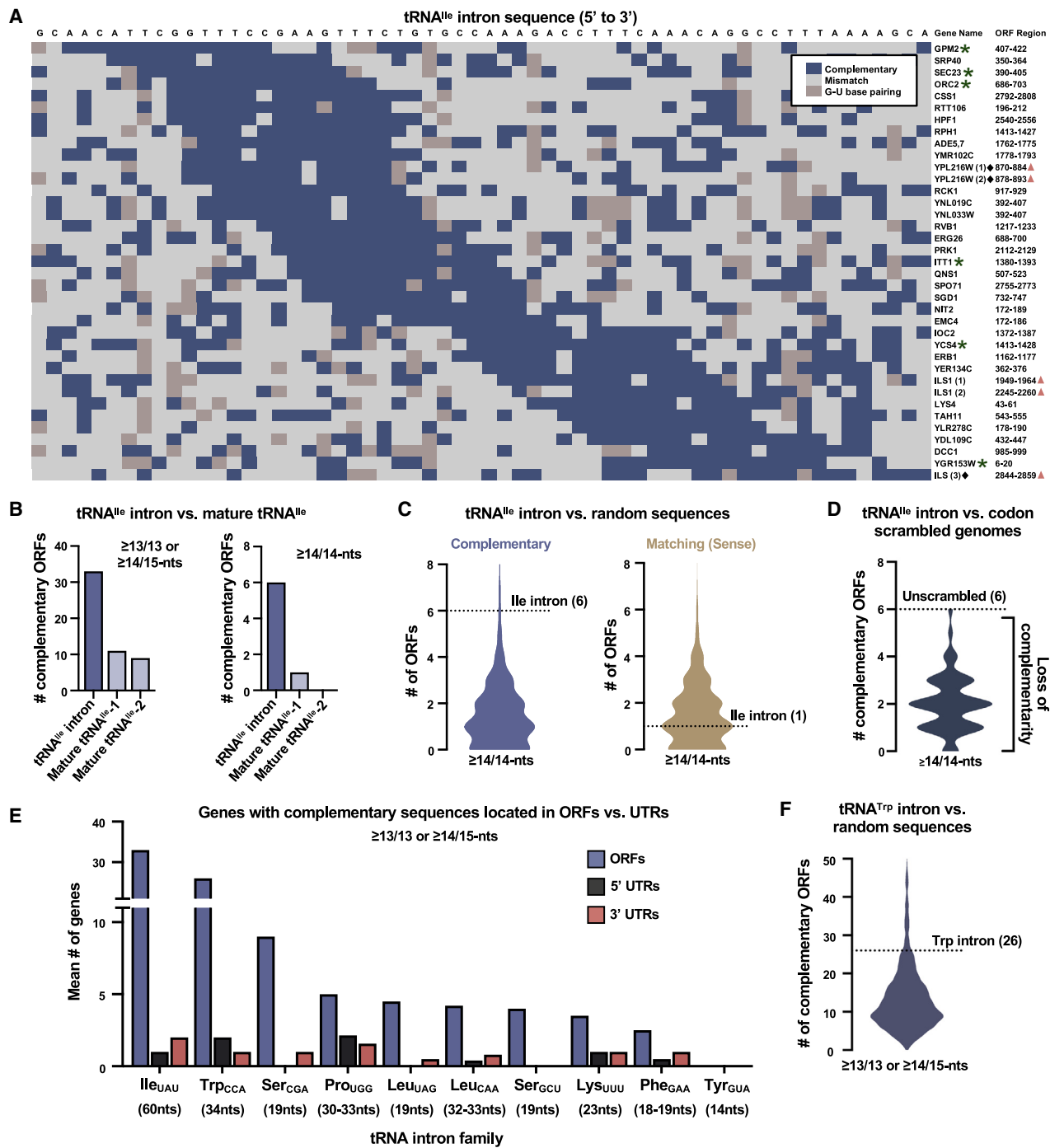


Figure 1. tRNA introns possess long stretches of complementarity to ORFs in *S. cerevisiae*

(A) Genes with ORF complementarity to the tRNA^{Ile} intron ($\geq 13/13$ or $\geq 14/15$ nt, before GU base pairing). ORF region: nucleotide position of complementarity. Green asterisks: $\geq 14/14$ nt complementarity. Pink triangles: >1 region of complementarity. Diamond: meets criteria only with GU base pairing.

(B) Number of complementary ORFs in tRNA^{Ile} intron vs. mature tRNA^{Ile}. tRNA^{Ile}-1: chromosome 4; tRNA^{Ile}-2: chromosome 12.

(C) Number of complementary (left) or matching (right) ORFs in 1,000 randomly generated sequences with the same length and GC content as the tRNA^{Ile} intron.

(D) Number of ORFs with complementarity to the tRNA^{Ile} intron in 100 randomly generated codon-scrambled genomes.

(legend continued on next page)

of tRNA introns, both within and between organisms. First, the number and percentage of intron-containing tRNA genes between organisms vary greatly. In humans, 7% of the approximately 400 tRNA genes contain an intron, whereas in the yeasts *S. cerevisiae* and *Cryptococcus neoformans* 22% (61/275) and 98% (132/135), respectively, of tRNA genes contain an intron.¹³ Second, tRNA intron length varies between and within species, ranging from 14 to 60 nt in *S. cerevisiae*, 12–24 nt in humans, and up to nearly 300 nt in other eukaryotes.¹³ Third, the number of intron-containing tRNA families varies between organisms. In *S. cerevisiae* and humans, there are ten and four intron-containing tRNA families, respectively.

Despite this variation, multiple lines of evidence support tRNA intron sequence conservation. First, in higher eukaryotes, as well as *S. cerevisiae*, all genes encoding a particular tRNA family within that organism often contain an intron with identical or nearly identical sequences. For example, the two tRNA^{Leu}_{UAU} genes in *S. cerevisiae* contain introns with identical sequences, whereas none of the tRNA^{Leu}_{AAU} genes contain an intron. Second, the tRNA families that contain introns in metazoans are similar.²⁶ Most of the tRNA^{Leu}_{CAA}, tRNA^{Leu}_{UAU}, and tRNA^{Tyr}_{GUA} genes contain introns in *Drosophila*, *C. elegans*, mice, and humans.²⁶ In fact, every tRNA^{Tyr}_{GUA} gene from all annotated eukaryotes contains an intron.¹³ Lastly, tRNA intron sequences are conserved in closely related species.²⁶ For example, the 113–119-nt tRNA^{Tyr}_{GUA} intron from 12 different species of Drosophilids, separated evolutionarily by about 50 million years, shows remarkable sequence and structural similarities.²⁴

Although the presence of introns in tRNA genes is unessential in *S. cerevisiae*,^{27,28} their conservation suggests they provide advantages to cells. A few reports hint at such roles. At the DNA level, tRNA introns can impact the ability of tRNA genes to serve as insulators for nearby genes²⁹ and protect against viral genome integration in archaea.³⁰ At the RNA level, the presence of introns within precursor tRNAs containing mutations in the anticodon stem-loop directs them for Met22-dependent pre-tRNA decay.³¹ Additionally, their presence can affect whether modification enzymes recognize an intron-containing tRNA³² and can prevent mismodification.²⁷

Although these reports identify potential advantages for maintaining introns in tRNA genes, they do not explain tRNA intron sequence conservation.^{24,26} One possibility is that excised, free tRNA introns function as sncRNAs, like microRNAs (miRNAs), which base pair to complementary mRNAs and mediate Argonaute (AGO)-dependent RNA silencing.³³ More recently, several noncanonical sncRNAs have been identified that are derived from post-transcriptional fragmentation of longer RNAs and function like miRNAs, such as tRFs.^{34–36}

Here, we investigated whether tRNA introns function as sncRNAs. Using bioinformatic, molecular, and genetic approaches, we demonstrate that free tRNA introns in *S. cerevisiae* base pair to target mRNA open reading frames

(ORFs), inducing mRNA decay. Furthermore, free tRNA intron levels are modulated by environmental stressors, such as oxidative stress, in tRNA family-specific manners, resulting in selective, complementarity-dependent regulation of mRNA levels. Thus, free introns of tRNAs (fitRNAs) are another member of the sncRNA family and mediate a previously unknown form of gene regulation.

RESULTS

tRNA introns possess remarkable complementarity to ORFs

If tRNA introns have a sequence-dependent biological function, sequence conservation among closely related species, as observed for the tRNA^{Tyr} intron in Drosophilids,^{24,26} would be expected. We conducted a similar sequence analysis in yeasts, using the two longest tRNA introns in *S. cerevisiae*, the tRNA^{Leu} and tRNA^{Trp} introns. These intron sequences are highly conserved, with nearly all of the intron sequences from the reiterated tRNA^{Leu} or tRNA^{Trp} genes in the *Saccharomyces* genus displaying >90% identity to the respective *S. cerevisiae* intron sequences (Table S1).

Given this sequence conservation, tRNA introns may function as sncRNAs base pairing to complementary sequences on mRNAs.³³ To determine whether tRNA introns exhibit such complementarity, we computationally searched the *S. cerevisiae* coding genome for mRNA ORFs possessing long stretches of complementarity to tRNA introns. Using the formula: 4ⁿ/yeast ORFome size, where $n = \#$ of consecutive nt, we can estimate the length of complementarity necessary to yield targets that would be highly improbable to occur by chance. For example, a random 13-, 14-, or 15-nt sequence would have a 13%, 3%, and 0.8% chance of appearing once in the yeast ORFome, respectively. Therefore, we used the criteria of a minimum of 13 nt perfect complementarity ($\geq 13/13$ nt) or 15 nt allowing for a single mismatch ($\geq 14/15$ nt) using standard Watson-Crick-Franklin base pairing rules. We identified 137 ORFs bearing complementarity to the 26 unique tRNA intron sequences (Table S2A). These genes were enriched relative to the total yeast genome for processes such as DNA replication, organelle, mitochondrial and chromatin organization, and meiotic/mitotic cell cycle (Figure S1A).

The 60-nt tRNA^{Leu}_{UAU} intron possesses complementarity to 33 different ORFs (Figure 1A; 6 ORFs at $\geq 14/14$ nt). These genes are enriched for chromatin and organelle organization, meiotic cell cycle, and transcription by RNA polymerase II (Figure S1B). The complementarity is evenly distributed throughout the intron (Figure 1A) and ORFs (Figure S1C) and is biased relative to matching (sense) sequences (Figure S1D). By contrast, the longer 73-nt mature tRNA^{Leu} possesses complementarity to considerably fewer ORFs (Figure 1B), indicating a majority of ORF complementarity to tRNA^{Leu} is restricted to the intron.

(E) Number of genes with $\geq 13/13$ or $\geq 14/15$ nt of complementarity in ORFs or UTRs for each intron-containing tRNA family. If >1 unique intron sequence, the mean number of complementarity-bearing genes is shown. Intron lengths are in parentheses.

(F) Same as (C, left), but for the tRNA^{Trp} intron.

(C, D, and F) Dotted line indicates the number of ORFs with complementary or matching sequences to the authentic tRNA^{Leu} or tRNA^{Trp} intron. See also Figures S1F and S2C and Tables S2.

To examine the probability that the extent of tRNA^{lle} intron complementarity to ORFs is occurring by chance, we generated 1,000 random sequences with the same length and GC content as the tRNA^{lle} intron. Of these, <2% had $\geq 14/14$ nt complementarity to more ORFs than the authentic tRNA^{lle} intron (Figures 1C and S1E for $\geq 13/13$ or $\geq 14/15$ nt). For comparison, 43% of randomly generated sequences displayed more ORFs with matching sequences than the authentic tRNA^{lle} intron (Figure 1C, right). These results indicate that the extent of tRNA^{lle} intron complementarity to ORFs is statistically improbable.

We next assessed the impact of the yeast codon sequence on the specificity of tRNA intron complementarity by calculating the number of ORFs with $\geq 14/14$ -nt tRNA^{lle} intron complementarity in 100 codon-scrambled genomes. Codon scrambling resulted in decreased complementarity in 98% of genomes, compared with unscrambled (Figure 1D). Thus, tRNA^{lle} intron complementarity has a strong dependency on the natural codon arrangement of the genome.

Like the tRNA^{lle} intron, the 34-nt tRNA^{Trp}_{CCA} intron displays remarkable complementarity ($\geq 13/13$ or $\geq 14/15$ nt) to 26 ORFs (Figures 1E and S1F). Overall, these genes are enriched for DNA recombination, replication, and repair; mitotic cell cycle; cell-cycle regulation; and transcription by RNA polymerase II (Figure S2A). Of 1,000 random computer-generated sequences with the same length and GC content as the tRNA^{Trp} intron, only 8% surpassed the authentic tRNA^{Trp} intron in number of complementary ORFs (Figure 1F). The tRNA^{Trp} intron also possesses greater complementarity than mature tRNA^{Trp}, despite being less than half the size (Figure S2B). Furthermore, the tRNA^{Trp} intron displays a 1.9-fold bias for complementary vs. matching ORFs (Figure S1D). Therefore, like the tRNA^{lle} intron, the tRNA^{Trp} intron sequence confers statistically improbable levels of complementarity to ORFs.

Except for the shortest 14-nt tRNA^{Tyr}_{GUA} intron, the remaining intron-containing tRNA families also possess ORF complementarity (Figures 1E and S2C; Table S2A). Furthermore, the tRNA introns exhibit greater complementarity to ORFs than to 5' and 3' UTRs combined (137 vs. 34; Figure 1E), despite typical UTR lengths of 50–200 nt in *S. cerevisiae*.³⁷

The results above demonstrate that tRNA introns possess substantial complementarity to ORFs. In particular, the extent of complementarity to the tRNA^{lle} and tRNA^{Trp} introns is exceptional relative to random sequences, matching sequences, mature tRNAs, UTRs, and other tRNA introns. Therefore, we investigated the biological roles of the tRNA^{lle} and tRNA^{Trp} introns on mRNAs bearing ORF complementarity.

Genomic tRNA^{lle} intron deletion increases mRNA levels for complementarity-bearing genes

To determine whether tRNA intron-ORF complementarity affects gene expression, we generated a yeast strain lacking the tRNA^{lle} introns (tRNA^{lle}i Δ) (Figure 2A). Successful deletion was confirmed by sequencing and northern blot analysis. Wild-type (WT) cells express several intron-containing tRNA^{lle} species, including the initial tRNA^{lle} transcript containing leader and trailer sequences (P), end-processed, intron-containing tRNA^{lle} (I), a likely exon-intron tRNA^{lle} fragment (two-thirds),³⁸ and free tRNA^{lle} intron (Figure 2B; lane 1). These species are absent in

the tRNA^{lle}i Δ strain (lane 2). Reverse-transcription quantitative PCR (RT-qPCR) analysis confirmed the absence of the tRNA^{lle} intron and unaltered levels of mature tRNA^{lle} (Figure 2C), as previously shown.²⁷

The tRNA^{lle}i Δ strain was employed to assess the effects of tRNA^{lle} intron loss on mRNA levels for complementarity-bearing genes. mRNA levels of nearly all genes (31/33) in Figure 1A were assessed by RT-qPCR in tRNA^{lle}i Δ and WT cells. In the tRNA^{lle}i Δ strain, mRNA levels for >75% of the genes (24/31) were elevated above WT levels (Figure 2D). These changes were also reflected at the protein level. tRNA^{lle}i Δ cells expressing C-terminally 6xHIS-tagged GPM2, whose ORF possesses 14-nt tRNA^{lle} intron complementarity (Figure 1A), showed a 40% increase in Gpm2-6xHIS protein levels relative to WT (Figure S3A,B), comparable to changes at the mRNA level (Figure 2D).

To determine whether the changes in mRNA levels in the tRNA^{lle}i Δ strain are due to tRNA^{lle} intron-ORF complementarity, we selected 28 genes that did not meet the criteria of $\geq 13/13$ - or $\geq 14/15$ -nt complementarity to the tRNA^{lle} intron. These genes include common yeast housekeeping genes (i.e., ACT1 and TDH1), genes with complementarity to other tRNA intron families (i.e., ATG5 has complementarity to the tRNA^{Trp} intron), paralogs of genes with complementarity (i.e., GPM1 and GPM3 are paralogs of GPM2), and other randomly selected genes. Although many of these genes have 6–12-nt stretches of complementarity to the tRNA^{lle} intron (Figure S3E), which may or may not have biological relevance, these genes do not meet our stringent complementarity criteria ($\geq 13/13$ or $\geq 14/15$ nt) and are herein termed as lacking complementarity.

Of these genes that lack tRNA^{lle} intron complementarity, mRNA levels for <35% (9/28) were elevated in the tRNA^{lle}i Δ strain relative to WT (Figure 2E). Again, these findings are supported at the protein level. Genes lacking tRNA^{lle} intron complementarity, specifically NSP1 and GSP1, displayed no change in protein levels in the tRNA^{lle}i Δ strain (Figures S3A and S3B). Interestingly, the collective changes in mRNA levels for all 28 genes lacking complementarity showed a small increase in the tRNA^{lle}i Δ strain relative to WT (Figure 2F). This may indicate that loss of tRNA^{lle} introns has a general stimulatory effect on cellular mRNA levels. Alternatively, cells lacking the tRNA^{lle} introns may have altered cellular mRNA, rRNA, and tRNA ratios, which could artificially increase mRNA levels when standardizing RT-qPCR data to total RNA. To account for these possibilities, all RT-qPCR analyses were performed by comparing mRNA levels of genes with complementarity to those without, rather than comparing mRNA levels between strains. As such, the increase in mRNA levels for complementarity-bearing genes was significantly greater than for genes without (Figure 2F). These data suggest that the tRNA^{lle} intron negatively regulates mRNA levels of genes bearing complementarity within their ORFs.

The complementarity-dependent inhibitory role of the tRNA^{lle} intron on mRNA levels resembles miRNA-mediated gene silencing. However, in mammalian cells, miRNAs canonically base pair to mRNA 3' UTRs.³⁹ To determine whether the tRNA^{lle} intron can also target the 3' UTR, we measured mRNA levels for all 11 genes with 3' UTR complementarity to the tRNA^{lle} intron at the less stringent parameter of $\geq 12/12$ or $\geq 13/14$ nt. The change in mRNA levels in the tRNA^{lle}i Δ strain was similar for

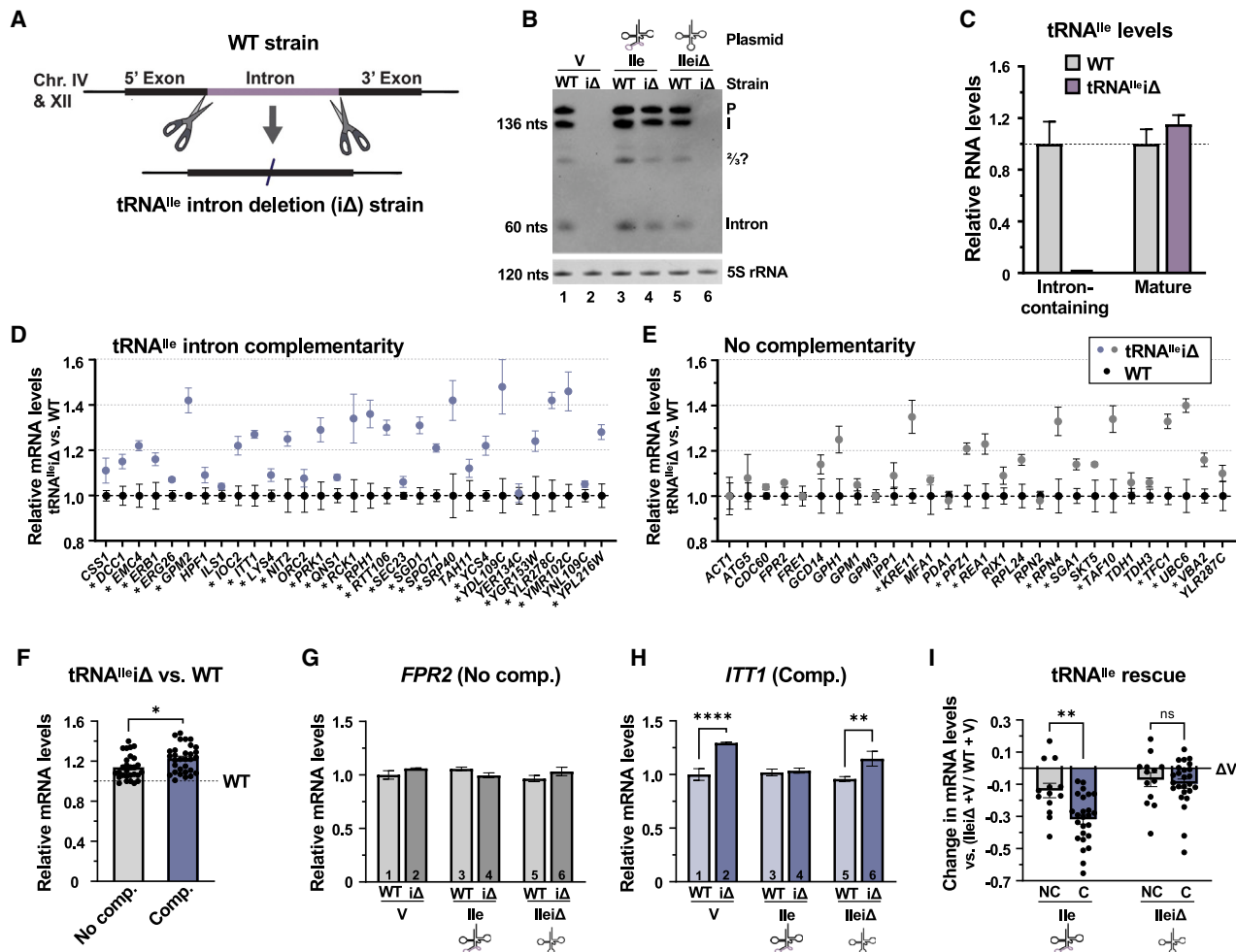


Figure 2. Genomic deletion of tRNA^{Ile} introns increases mRNA levels for complementarity-bearing genes

(A) Strategy for generating a tRNA^{Ile} $i\Delta$ strain, lacking the two copies of the tRNA^{Ile} intron from chromosomes 4 and 12.

(B) Northern blot analysis of wild-type (WT) or tRNA^{Ile} $i\Delta$ ($i\Delta$) strains containing vector only (V; lanes 1–2), intron-containing tRNA^{Ile} low-copy plasmid (Ile; lanes 3–4), or intron-less tRNA^{Ile} plasmid (Ile Δ ; lanes 5–6). Blots probed with oligonucleotide complementary to tRNA^{Ile} intron. P: 5' leader, I: end-processed intron-containing tRNA^{Ile}; 2/3ds: likely tRNA^{Ile} intron plus either 5' or 3' exon.

(C) Intron-containing and mature tRNA^{Ile} levels in WT or tRNA^{Ile} $i\Delta$ cells. $n = 6$.

(D and E) mRNA levels of genes with (D) or without (E) tRNA^{Ile} intron complementarity in WT or tRNA^{Ile} $i\Delta$ cells. Black dots: WT mRNA levels, set to 1; blue or gray dots: tRNA^{Ile} $i\Delta$ mRNA levels. $n = 5$. The false discovery rate was controlled separately for (D) and (E) using the Benjamini, Krieger, and Yekutieli method. * $p < 0.05$.

(F) Summary graph of changes in mRNA levels with each dot representing a different gene shown in (D) and (E).

(G and H) FPR2 (G) and ITT1 (H) mRNA levels for WT and tRNA^{Ile} $i\Delta$ cells containing plasmids in (B). $n = 5$.

(I) Summary graph of mRNA levels from tRNA^{Ile} rescue experiment. Each dot represents a different gene from (G) and (H) and Figures S4 and S5. Data expressed as mRNA levels in tRNA^{Ile} $i\Delta$ strain relative to WT. The change in mRNA levels with vector (ΔV) is set to 1. NC, no complementarity; C, complementarity. RNA levels in all graphs measured by RT-qPCR. For (C) and (F)–(H), data expressed relative to WT or WT + V, set to 1. Data in all graphs are expressed as mean \pm SEM. For (F–I), * $p < 0.05$; ** $p < 0.01$; *** $p < 0.0001$; ns: $p > 0.05$. See also Figure S3.

genes with and without 3' UTR complementarity (Figures S3C and S3D). In support of our bioinformatic analysis, the data indicate that the ORF, and not the 3' UTR, is a key site for tRNA^{Ile} intron complementarity-dependent regulation of mRNA levels.

To gain insights into the “rules of complementarity,” we performed linear regression analyses to correlate the magnitude of changes in mRNA levels for genes with complementarity to factors such as the extent and location of complementarity. There was no correlation between the magnitude of changes in

mRNA levels in the tRNA^{Ile} $i\Delta$ strain and the largest number of consecutive complementary nucleotides (Figure S3E) or the location of complementarity, either within the ORF (Figure S3F) or within the intron (Figure S3G).

To verify that the increased mRNA levels in the tRNA^{Ile} $i\Delta$ strain for complementarity-bearing genes are indeed due to the lack of intron, WT and tRNA^{Ile} $i\Delta$ cells were transformed with yeast plasmids possessing the tRNA^{Ile} gene with (tRNA^{Ile}) or without (tRNA^{Ile} $i\Delta$) the intron. Successful expression of tRNA^{Ile} or tRNA^{Ile} $i\Delta$

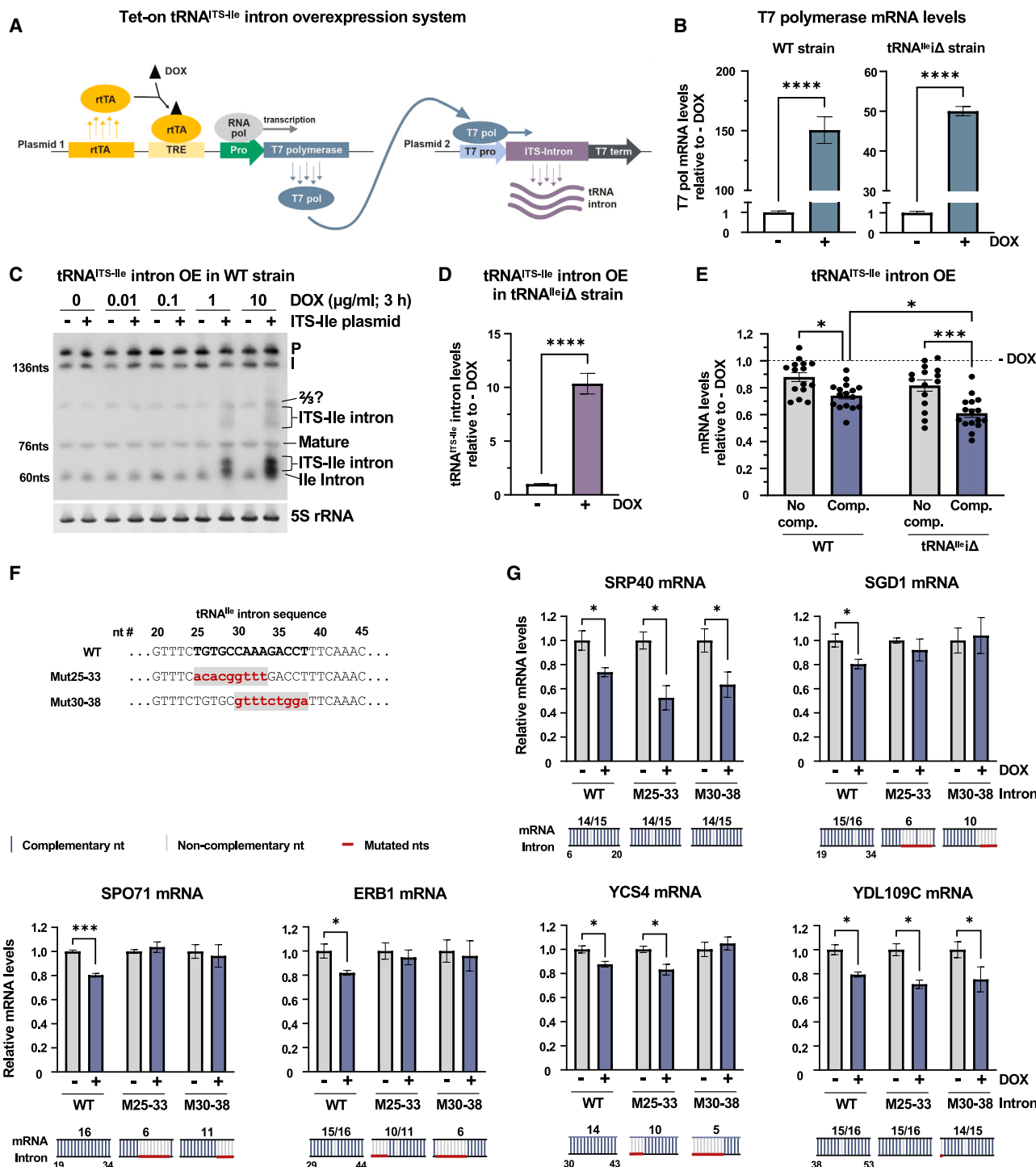


Figure 3. Inducible overexpression of tRNA^{ITS-IIe} intron decreases mRNA levels for complementarity-bearing genes

(A) Two-plasmid tet-on system for overexpressing (OE) tRNA^{ITS-IIe} intron. rtTA, reverse tetracycline transactivator; DOX, doxycycline; TRE, tetracycline-responsive element; RNA Pol II, RNA polymerase II; Pro, CYC1 promoter.

(B) T7 polymerase mRNA levels in WT and tRNA^{IIe}Δ cells following 10 μg/mL DOX treatment (+) or vehicle (-) for 4 h in cells expressing plasmid #1. $n = 4$.

(C) Northern blot showing tRNA^{ITS-IIe} intron overexpression in WT cells expressing plasmid #1 and vector (-) or tRNA^{ITS-IIe} plasmid (+) following 3 h DOX treatment at indicated concentrations. Blot was probed with oligonucleotides complementary to tRNA^{IIe} intron and mature tRNA^{IIe}. P, I, and 2/3rds bands are described in Figure 2B.

(D) tRNA^{ITS-IIe} intron levels in tRNA^{IIe}Δ strain treated with 10 μg/mL DOX for 3 h. $n = 4$.

(legend continued on next page)

was confirmed by northern blot analysis (Figure 2B, lanes 3–6). If the increases in mRNA levels in the tRNA^{Ile}iΔ strain are due to the lack of tRNA^{Ile} intron, then expression of a plasmid containing the tRNA^{Ile} gene with the intron should suppress this effect, resulting in mRNA levels similar to WT. Conversely, a plasmid containing the tRNA^{Ile} gene lacking the intron should be unable to suppress this effect, resulting in mRNA levels similar to those in the tRNA^{Ile}iΔ strain. For genes lacking complementarity, mRNA levels should not be affected by either tRNA^{Ile}. Accordingly, mRNA levels of a gene lacking tRNA^{Ile} intron complementarity, *FPR2*, were unchanged in the tRNA^{Ile}iΔ strain relative to WT when expressing the vector alone (V), tRNA^{Ile} plasmid, or tRNA^{Ile}iΔ plasmid (Figure 2G). For *IT71*, which contains 14-nt tRNA^{Ile} intron complementarity, the intron-containing tRNA^{Ile} plasmid rescued the increase in mRNA levels observed in the tRNA^{Ile}iΔ strain expressing the vector alone (Figure 2H, columns 1 and 2 vs. 3 and 4). Conversely, the tRNA^{Ile}iΔ plasmid was unable to rescue mRNA levels (Figure 2H, columns 1 and 2 vs. 5 and 6). The data support the role of the tRNA^{Ile} intron in modulating *IT71* mRNA levels.

We expanded these plasmid rescue studies to include a larger number of genes with and without complementarity (Figures S4 and S5). Two-way ANOVA demonstrates a statistically significant interaction between the plasmid and complementarity ($F(2,108) = 7.181; p = 0.0012$). More specifically, as compared with vector, expression of the tRNA^{Ile} plasmid significantly decreased mRNA levels in the tRNA^{Ile}iΔ strain for genes with complementarity vs. genes without (Figure 2I, left). Conversely, when the tRNA^{Ile}iΔ plasmid was expressed, the change in mRNA levels was similar for genes with and without complementarity (Figure 2I, right). Together, these data demonstrate that the tRNA^{Ile} intron can rescue changes in mRNA levels in a tRNA^{Ile}iΔ strain, specifically for genes with complementarity, supporting a role of the tRNA^{Ile} intron in complementarity-dependent inhibition of mRNA levels.

Inducible tRNA^{Ile} intron overexpression elicits complementarity-dependent decreases in mRNA levels

Although the data obtained using the tRNA^{Ile}iΔ strain indicate that tRNA intron-ORF complementarity decreases mRNA levels, they cannot distinguish between effects mediated by free intron or intron-containing tRNA precursors. In addition, the absence of tRNA^{Ile} introns prevents normal pseudouridylation of pre-tRNA^{Ile} at anticodon positions 34 and 36, resulting in mismodification of 40% of U₃₄ in mature tRNA^{Ile} to ncm⁵U.²⁷ The ncm⁵UAU anticodon does not misdecode AUG codons as Ile,²⁷ but this mismodification could have other cellular impacts. Therefore, to specifically address whether free tRNA introns can downregulate mRNA levels for complementarity-bearing genes, we developed a tet-on system to induce tRNA^{Ile} intron overexpression (Figure 3A).

Briefly, cells were transformed with two plasmids. The first contains the genes for the reverse tetracycline transactivator

(rtTA) under a constitutive promoter and a nuclear localization signal (NLS)-containing T7 polymerase under the control of a tetracycline-responsive element (TRE). Following doxycycline (DOX) treatment, rtTA binds the TRE, inducing RNA polymerase II-mediated T7 polymerase transcription. Accordingly, 4 h exposure to 10 µg/mL DOX elicits a ≥50-fold increase in T7 polymerase mRNA levels in WT and tRNA^{Ile}iΔ cells (Figure 3B).

The second plasmid contains DNA encoding the tRNA^{Ile} intron under the control of a T7 promoter and terminator (Figure 3A). The intron was modified to contain a 5' GGGAGA sequence, known as the initially transcribed sequence (ITS), to enhance transcription (Figure S6A)^{40,41} and is herein referred to as the tRNA^{ITS-Ile} intron. To decrease read-through transcription by T7 polymerase,^{42,43} the T7 terminator sequence was also modified (Figures S6B and S6C). In response to 3 h DOX treatment, northern blot analysis showed a dose-dependent increase in tRNA^{ITS-Ile} intron expression in WT cells, detectable at concentrations of ≥1 µg/mL DOX and similar in size to the authentic tRNA^{Ile} intron (Figure 3C). At the highest dose, tRNA^{ITS-Ile} intron levels increased 10-fold in tRNA^{Ile}iΔ cells (Figure 3D).

Unlike the endogenous tRNA^{Ile} intron that is generated in the cytoplasm in *S. cerevisiae*,^{20,21} the tRNA^{ITS-Ile} intron is transcribed by a nuclear T7 polymerase. However, its small size should allow for passive diffusion to the cytoplasm.⁴⁴ This was confirmed by subcellular fractionation experiments. Yeast cells treated for 0–3.5 h with DOX were fractionated into cytoplasmic and organellar fractions (Figure S6D). Fraction purity was verified by western blotting using antibodies against Nup1 (nuclear) and Atp2 (mitochondrial) for the organellar fraction and Rna1 for the cytoplasmic fraction. Northern blot analysis revealed similar levels of tRNA^{ITS-Ile} intron in the organellar fraction following 2 and 3.5 h of DOX. By contrast, tRNA^{ITS-Ile} intron levels increased from 2 to 3.5 h in the cytoplasmic fraction, consistent with intron re-localization from the nucleus to the cytoplasm.

Using the tet-on tRNA^{ITS-Ile} intron overexpression system, we assessed mRNA levels for genes with and without tRNA^{Ile} intron complementarity following DOX treatment. For genes without complementarity, DOX induced a 12% decrease in mRNA levels in WT cells (Figures 3E and S7A), whereas genes with complementarity displayed a 26% decrease (Figures 3E and S7B). We anticipated that the magnitude of changes would be greater in the tRNA^{Ile}iΔ strain due to absence of endogenous tRNA^{Ile} intron. Indeed, genes without and with complementarity were decreased by 18% and 39%, respectively, in cells lacking the genomic tRNA^{Ile} introns (Figures 3E, S7C, and S7D). This demonstrates that free tRNA^{ITS-Ile} intron negatively regulates mRNA levels in a complementarity-dependent manner.

The requirement of complementarity implies a direct interaction between the tRNA^{Ile} intron and its targets. To address this experimentally, we overexpressed the tRNA^{ITS-Ile} intron

(E) Summary graph of changes in mRNA levels for genes with and without tRNA^{Ile} intron complementarity in WT and tRNA^{Ile}iΔ cells, following 4 h 10 µg/mL DOX. Each dot represents mean mRNA levels for a different gene, shown in Figures S7A–S7D. $n = 5$.

(F) WT and mutant tRNA^{ITS-Ile} intron sequences. Red: mutated nucleotides.

(G) mRNA levels in WT cells expressing WT or mutant tRNA^{ITS-Ile} intron, following 3 h 10 µg/mL DOX. Drawings below graphs indicate positions of intron mutations (red) with maximum complementarity indicated above drawing. For all graphs, mRNA levels measured by RT-qPCR and expressed relative to –DOX, set as 1. All cells contain plasmids #1 and #2, unless indicated otherwise. Data in all graphs are expressed as mean ± SEM. * $p < 0.05$; ** $p < 0.001$; *** $p < 0.0001$. See also Figure S7.

bearing short stretches of nucleotide substitutions and assessed DOX-induced changes in mRNA levels for six target ORFs, two of which maintain complementarity to the mutated introns and four of which have partial disruption of complementarity. In the tRNA^{ITS-IIe(M25-33)} and tRNA^{ITS-IIe(M30-38)} introns, nt 25-33 or 30-38 of the tRNA^{IIe} intron, respectively, were changed to the complementary nucleotides (Figures 3F and S7E). Both mutated tRNA^{ITS-IIe} introns are expressed in response to DOX treatment; however, the banding patterns observed by northern blot analysis differ from WT, despite bearing only nucleotide substitutions (Figure S7F). Therefore, we quantified the total amount of WT and mutant tRNA^{ITS-IIe} intron following DOX treatment by RT-qPCR using primers that specifically detect the exogenously overexpressed intron, but not endogenous tRNA^{IIe} intron or intron-containing tRNA^{IIe} precursors. WT and mutant tRNA^{ITS-IIe} intron levels increased 13-fold following DOX treatment (Figure S7G), resulting in decreased mRNA levels for genes with undisrupted complementarity (*SRP40* and *YDL109C*) (Figure 3G). Conversely, overexpression of the mutant tRNA^{ITS-IIe} introns failed to decrease mRNA levels for genes with substantially disrupted complementarity (*SGD1*, *SPO71*, *ERB1*, and *YCS4*). These data demonstrate direct interactions between the tRNA^{ITS-IIe} intron and complementary targets.

Since the inhibitory effect of tRNA introns requires base pairing to target sequences, these targets theoretically could be DNA or mRNA, leading to decreased transcription or transcript stability, respectively. To assess the latter possibility, we overexpressed the tRNA^{ITS-IIe} intron in yeast cells bearing deletions or temperature-sensitive (ts) mutations in components of different RNA decay pathways: the nuclear or cytoplasmic 5'-3' exonucleases, Rat1 and Xrn1, respectively, and the RNA exosome components Dis3, Rrp6, and Ski7.⁴⁵⁻⁴⁷ To ensure that any effects in these strains are due to impaired mRNA turnover, we measured tRNA^{ITS-IIe} intron levels following DOX treatment. Surprisingly, tRNA^{ITS-IIe} intron levels varied greatly between the mRNA decay-defective strains. For example, *rrp6Δ* and *xrn1Δ* cells displayed 7- and 5-fold increases, respectively, in tRNA^{ITS-IIe} intron levels upon DOX treatment, compared with 13-fold in WT cells, whereas *ski7Δ* cells failed to accumulate intron (Figure S7H). Therefore, these strains were not used for further analysis. Conversely, *dis3-1* and *rat1-1* cells grown at the non-permissive temperature displayed 56- and 20-fold increases in tRNA^{ITS-IIe} intron levels, respectively, compared with 11-fold in WT (Figure 4A). Therefore, the absence of a DOX-induced decrease in mRNA levels would indicate the involvement of the mutated RNA decay component.

In *rat1-1* cells grown at the non-permissive temperature, the decrease in mRNA levels following DOX treatment was abolished for 8/9 genes tested (Figure 4B). In *dis3-1* cells, 5/9 genes displayed no decrease in mRNA levels upon DOX treatment. For some of these genes, the decrease in mRNA levels was inhibited in both *rat1-1* and *dis3-1* cells, but none of the genes displayed decreases in mRNA levels in both strains (Figure 4C). Together, these results support tRNA^{ITS-IIe} intron interactions with mRNA leading to decay via 5'-3' exonuclease and/or 3'-5' exosome pathways.

Endogenously generated free tRNA^{IIe} and tRNA^{Trp} introns mediate complementarity-dependent decreases in mRNA levels

The tRNA^{ITS-IIe} intron overexpression experiments support a role of free tRNA^{IIe} intron (fitRNA^{IIe}). However, the functionality of the intron-containing tRNA^{IIe} cannot be eliminated. Furthermore, overexpressed tRNA^{ITS-IIe} intron differs from endogenous, cytoplasmically generated fitRNA^{IIe}, as it is nuclearly transcribed and contains extra 5' and 3' sequences. Given these limitations, we designed experiments that would address whether complementarity-dependent downregulation of mRNA levels is mediated by (1) endogenously generated fitRNA^{IIe}, (2) intron-containing tRNA^{IIe}, and (3) introns from other tRNA families, specifically tRNA^{Trp}.

We utilized yeast strains with gene deletions or mutations that result in the accumulation of free tRNA introns and/or intron-containing tRNA precursors, without noticeable changes in mature tRNA levels,^{6,48} and measured mRNA levels for genes with and without tRNA^{IIe} and tRNA^{Trp} intron complementarity. First, we assessed a yeast strain that lacks the *TOM70* gene, which encodes a mitochondrial outer membrane protein required for efficient SEN complex localization to the mitochondrial surface.²⁰ Since *tom70Δ* cells are viable, tRNA splicing still occurs, albeit inefficiently, as evidenced by the accumulation of intron-containing tRNAs (Figures 5A and S8A). fitRNA^{IIe} and fitRNA^{Trp} levels are also increased by 44% and 78%, respectively. mRNA levels in *tom70Δ* cells for genes lacking complementarity were decreased by 27% vs. WT (Figures 5B and S8B). Genes with complementarity to the tRNA^{IIe} or tRNA^{Trp} introns showed an additional 16% decrease in mRNA levels (Figures 5B, S8C, and S8D). These results indicate that endogenous fitRNA^{IIe} and fitRNA^{Trp} and/or their intron-containing precursors elicit complementarity-dependent decreases in mRNA levels.

The findings for the tRNA^{IIe} intron in the *tom70Δ* strain are consistent with results obtained using the tRNA^{IIe}*iΔ* strain. First, changes in mRNA levels in *tom70Δ* cells for genes bearing tRNA^{IIe} intron complementarity negatively correlated with changes observed in the tRNA^{IIe}*iΔ* strain to a significantly greater extent than genes lacking complementarity (Figure S8E). Second, as observed in the tRNA^{IIe}*iΔ* strain, mRNA levels in *tom70Δ* cells for genes bearing tRNA^{IIe} intron complementarity in the 3' UTR were not different from those lacking complementarity (Figure S8F).

Accumulation of intron-containing tRNAs and fitRNAs is also observed in yeast that lack the *LOS1* gene. Los1 is one of three nuclear exporters, along with Crm1 and the Mex67-Mtr2 heterodimer, that traffics pre-tRNAs to the cytoplasm.⁴⁹ Accordingly, in *los1Δ* cells, intron-containing tRNAs accumulate (Figure 5C) in the nucleus.^{50,51} fitRNA^{IIe} and fitRNA^{Trp} levels are also elevated 4- to 5-fold (Figure 5C). mRNA levels for genes lacking complementarity to the tRNA^{IIe} or tRNA^{Trp} introns were similar in *los1Δ* and WT cells (Figures 5D and S8G). However, mRNA levels for genes bearing complementarity were decreased by 30% (Figures 5D, S8H, and S8I).

Although cells deficient in Tom70 and Los1 could impact mRNA levels by a pathway unrelated to tRNA intron accumulation, this is highly unlikely given that (1) Tom70 and Los1 function in very different aspects of tRNA biology, (2) the changes in mRNA levels are dependent on complementarity to two different

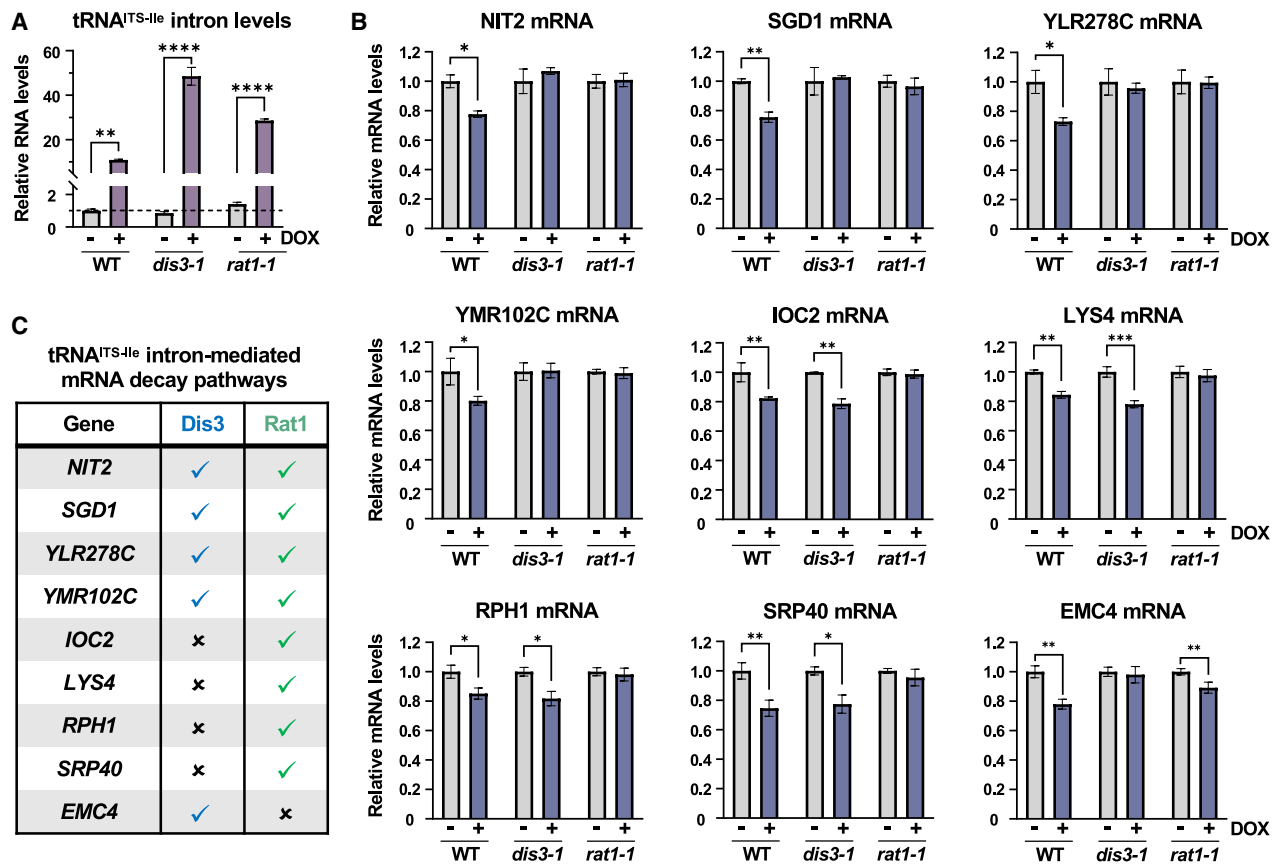


Figure 4. Disruption of RNA decay suppresses complementarity-dependent inhibitory effects of tRNA^{ITs-IIe} intron on mRNA levels

(A and B) tRNA^{ITs-IIe} intron levels (A) and mRNA levels (B) in strains with temperature-sensitive mutations in genes for RNA decay components. RNA levels expressed relative to –DOX in WT cells (A) or –DOX for each strain (B), set as 1. Cells were shifted to 37°C for 4 h. 10 µg/mL DOX was added after 1 h. All RNA levels were measured by RT-qPCR.

(C) Summary table of results from (B). Check marks indicate that the decrease in mRNA levels in WT cells is suppressed in the mutant strain. X indicates lack of suppression.

Data in all graphs are expressed as mean ± SEM. *p < 0.05; **p < 0.01; ***p < 0.001; ****p < 0.0001.

tRNA introns and are not observed for genes lacking complementarity, and (3) the data obtained with the *tom70Δ* and tRNA^{IIe}*iΔ* strains are consistent.

Since *tom70Δ* and *los1Δ* cells accumulate both fitRNAs and end-processed intron-containing tRNAs (Figures 5A and 5C), these effects could be mediated by either or both of these tRNA species. Therefore, we analyzed mRNA levels for genes with and without complementarity in yeast bearing ts mutations in the gene for the essential Sen2 subunit of the SEN complex. When shifted to the non-permissive temperature for 3 h, *sen2-1* cells display severe defects in tRNA splicing, resulting in the accumulation of end-processed intron-containing tRNAs and decreases in free introns (Figure 5E). mRNA levels in *sen2-1* cells for genes bearing complementarity to the tRNA^{IIe} and tRNA^{Trp} introns are elevated compared with genes lacking complementarity (Figures 5F and S8J–S8L). Since *sen2-1* cells accumulate end-processed intron-containing tRNAs, but no detectable free intron at the non-permissive temperature, these effects are likely mediated by the absence of fitRNA^{IIe} and fitRNA^{Trp}.

The role of the free intron is further supported by the lack of change in mRNA levels in *tom70Δ* cells for genes bearing complementarity overlapping the 5' exon-intron or intron-3' exon junction, as compared with those without (Figures S8M and S8N). Together, the results from the *los1Δ*, *tom70Δ*, and *sen2-1* strains indicate that endogenous fitRNA^{IIe} and fitRNA^{Trp}, but not their intron-containing precursors, are responsible for complementarity-dependent decreases in mRNA levels.

Oxidative stress induces accumulation of free tRNA^{Trp} intron and decreases in mRNA levels for complementarity-bearing genes

To determine whether complementarity-dependent tRNA intron-mediated gene regulation functions as a cellular stress response, we exposed *S. cerevisiae* to a variety of stressors and assessed fitRNA accumulation (results to be provided in a future publication). Our analysis revealed that treatment with hydrogen peroxide (H₂O₂) to induce oxidative stress elicited a >15-fold

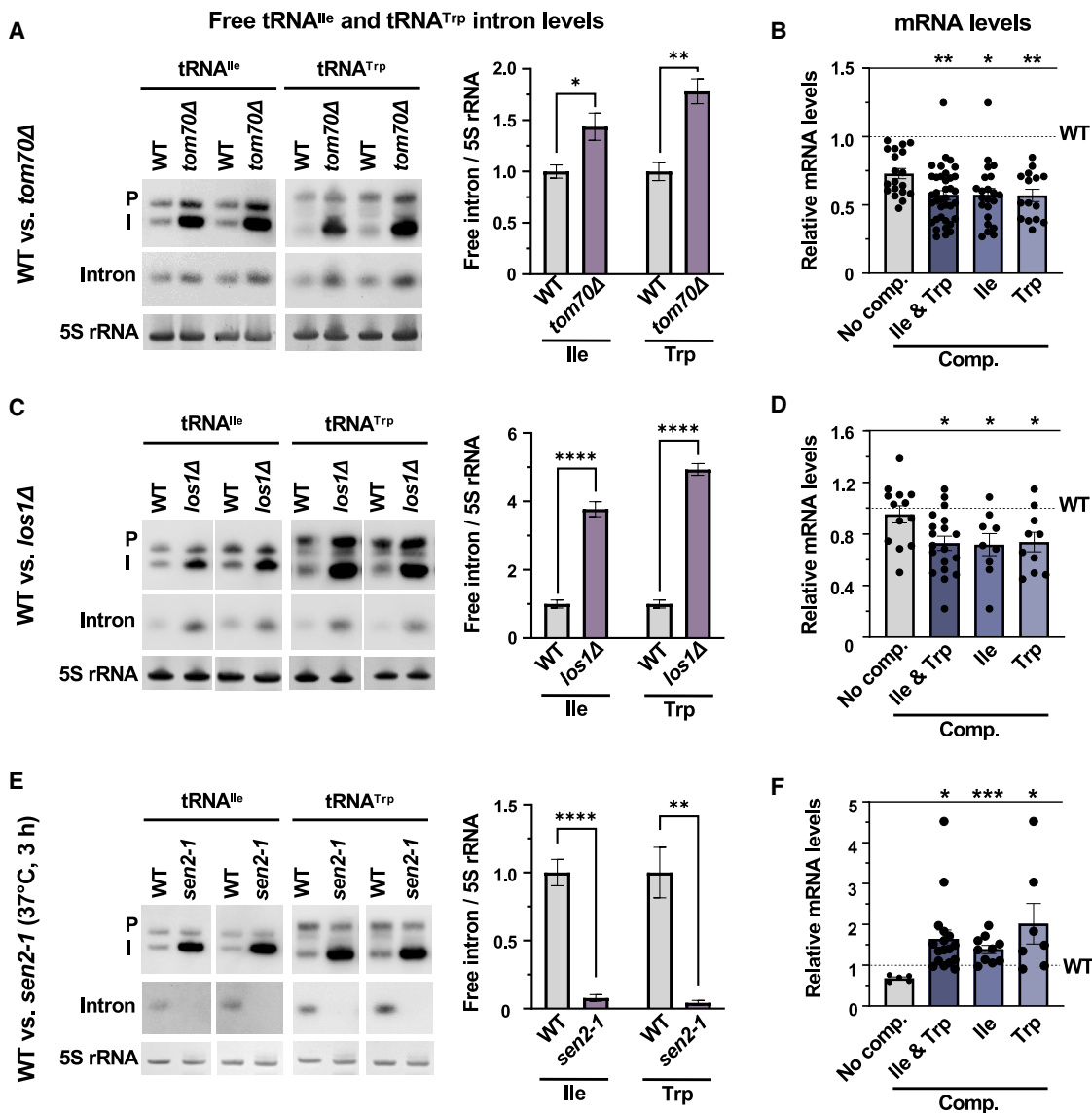


Figure 5. Accumulation of endogenous free tRNA^{Ile} and tRNA^{Trp} intron, but not their intron-containing tRNAs, decreases mRNA levels for complementarity-bearing genes

(A, C, and E) Representative northern blots (left) showing precursor tRNA^{Ile} and tRNA^{Trp} levels (P and I; described in Figure 2B) and free intron in WT and *tom70Δ* (A), *los1Δ* (C), and *sen2-1* (E) strains. Blots were probed with oligonucleotide complementary to tRNA^{Ile} or tRNA^{Trp} intron. All cultures grown at 23°C, except in (E) cultures, were shifted to 37°C for 3 h. Northern blot quantitation is shown on right. Data expressed relative to 5S rRNA levels, with WT set as 1. See Figure S8A for full-length blots of (A). n = 5.

(B, D, and F) mRNA levels, measured by RT-qPCR, in WT and *tom70Δ* (B), *los1Δ* (D), and *sen2-1* (F) cells for genes lacking or possessing tRNA^{Ile} intron and/or tRNA^{Trp} intron complementarity. Each dot represents mean mRNA levels for a different gene (see Figures S8B–S8D and S8G–S8L). Data expressed as mRNA levels in mutants relative to WT, set to 1.

Data in all graphs are expressed as mean ± SEM. *p < 0.05; **p < 0.01; ***p < 0.001; ****p < 0.0001.

increase in fitRNA^{Trp} levels relative to untreated cells (Figures 6A and 6B, pink), which was long-lived and dose-dependent (Figure S9A). Conversely, levels of pre-tRNA^{Trp} containing either the 5' leader and/or 3' trailer (P¹ and P²) dropped precipitously after 30 min, consistent with a rapid shutdown of new pre-tRNA^{Trp} synthesis (Figures 6A and S9A).

Interestingly, this effect was tRNA family specific, as only one other intron-containing tRNA family, tRNA^{Leu}_{CAA}, accumulated substantial free intron in response to H₂O₂ (Figures 6B orange, S9A, and S9B). The fitRNAs from three other tRNA families, tRNA^{Phe} (purple), tRNA^{Ser}_{GCU} (teal), and tRNA^{Lys} (yellow), displayed modest accumulation upon H₂O₂ treatment, whereas

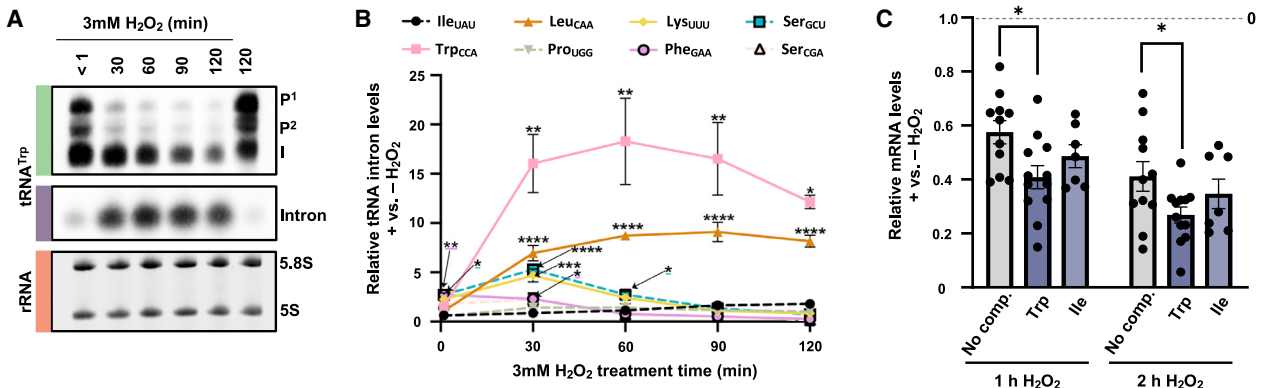


Figure 6. Oxidative stress triggers increased fitRNA^{Trp} and decreased mRNA levels for complementarity-bearing genes

(A) Representative northern blot showing levels of precursor tRNA^{Trp} (P¹, initial transcript; P², initial transcript containing 5' leader⁵² [denoted by green bar]); I, intron-containing end-processed pre-tRNA (green bar) or free intron (purple bar). Blots were probed with oligonucleotide complementary to tRNA^{Trp} intron. 5.8S and 5S rRNA (orange bar) serve as loading controls. WT cells were treated with 3 mM hydrogen peroxide (H₂O₂) for <1–120 min. Untreated cells were harvested at the same time as 2-h-treated cells.

(B) Quantitation of fitRNA levels from northern blots, as in (A) and Figure S9B. Data expressed relative to untreated cells, set as 1. n = 3.

(C) mRNA levels for genes with or without tRNA^{Trp} or tRNA^{Ile} intron complementarity, measured by RT-qPCR, following 3 mM H₂O₂. mRNA levels expressed relative to untreated cells (0 h), set to 1. Each dot represents mean mRNA levels for a different gene (see Figures S9C–S9E). n = 5. Data in all graphs are expressed as mean ± SEM. *p < 0.05; **p < 0.01; ***p < 0.001; ****p < 0.0001.

the remaining tRNA families showed no intron accumulation (Figures 6B, S9A, and S9B).

We measured mRNA levels following 1 and 2 h of 3 mM H₂O₂ treatment and found genes bearing tRNA^{Trp} intron complementarity were significantly reduced relative to those lacking complementarity (Figures 6C, S9C, and S9D). Conversely, mRNA levels for genes bearing tRNA^{Ile} intron complementarity showed no statistical difference from genes lacking complementarity (Figures 6C and S9E). Together, these results indicate that oxidative stress-induced accumulation of fitRNA^{Trp} mediates decreased mRNA levels for complementarity-bearing genes. Thus, fitRNAs not only function as complementarity-dependent, constitutive negative regulators of the transcriptome but likely function in cellular responses to stress.

DISCUSSION

Sequence conservation is a reliable indicator of biological significance. Yet sequence-dependent functions of tRNA introns, which are conserved features of tRNA genes dating back ~1,750 million years,⁵³ have been an enigma. Here, we demonstrate that excised tRNA introns constitute a previously unknown class of small regulatory RNAs. Akin to other classes of tRFs,¹ fitRNAs exploit target RNA complementarity to modulate gene expression.

Under standard growth conditions, fitRNAs may fine-tune expression of complementarity-bearing transcripts (Figure 7), as exemplified by the small reciprocal changes in mRNA levels upon fitRNA deletion (Figure 2F) or overexpression, demonstrated through the use of the tRNA^{ITS-Ile} intron (Figure 3E) or *tom70Δ* and *los1Δ* cells (Figure 5), as well as the enhanced effects of intron overexpression in the tRNA^{Ile}iΔ background (Figure 3E). Any change is noteworthy given the rapid and efficient turnover of fitRNAs (Figure S9B) and the potentially large number of fitRNA targets (Table S2). Importantly, the functions of fitRNAs

appear to be enhanced upon exposure to some stressors and used as cellular responses to downregulate specific transcripts (Figure 7). Given the substantial resources dedicated to transcribing, splicing, and degrading tRNA introns, we speculate that these constitutive and inducible functions of fitRNAs provide an advantage to cells. Such a payoff may account for the conservation of intron sequences in tRNA genes from archaea to humans over many millions of years. Indeed, we identified over 100 human ORFs that exhibit ≥13-nt complementarity to the 28 high-confidence human tRNA intron sequences (Table S3), suggesting fitRNAs could function similarly in other organisms.

fitRNAs role in post-transcriptional regulation

The inhibitory role of fitRNAs on mRNA levels depends on complementarity, as there is an inverse relationship between levels of fitRNAs and their respective complementary mRNAs (Figures 2F, 3E, 5B, 5D, 5F, and 6C). However, target RNA sensitivity to fitRNAs is likely dictated by more than just complementarity and may include factors such as local structure, copy number, sequence composition, subcellular locale, and translation status. First, only free tRNA introns, and not their intron-containing precursors, appear to mediate inhibitory effects on mRNA levels for complementarity-bearing genes (Figures 5E, 5F, and S8N). Second, genes with complementarity located within the 3' UTR were not impacted by fitRNA levels (Figures S3D and S8F). Third, even when complementarity was localized within ORFs, the effect on mRNA levels varied across individual genes. Of particular note, mRNA levels of *ILS1*, which possesses three distinct regions of ≥14/15-nt complementarity to the tRNA^{Ile} intron, were unaffected by alteration of fitRNA^{Ile} levels under all conditions tested (Figures 2D, S4, S7B, S7D, and S8D). Thus, complementarity-dependent mechanisms that function at the level of translation rather than mRNA stability may also be at play.

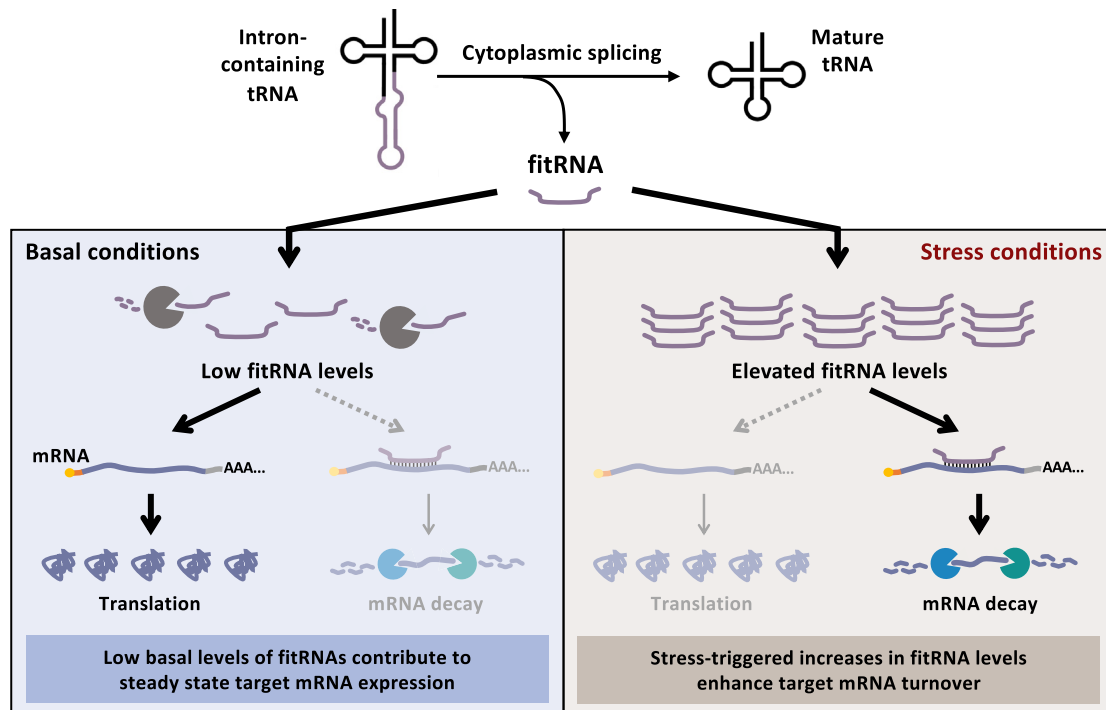


Figure 7. Model of complementarity-dependent constitutive and stress-induced functions of fitRNAs in *S. cerevisiae*

Cytoplasmic splicing of intron-containing tRNAs generates mature tRNAs and fitRNAs. Under basal conditions, fitRNAs are largely degraded in the cytoplasm, resulting in minor contributions to repression of target gene expression. Following cellular stress, family-specific fitRNA accumulation, due to decreased fitRNA turnover, leads to increased fitRNA-mRNA base pairing and subsequent mRNA degradation to downregulate stress-specific transcriptomes.

Conversely, small changes in mRNA levels were observed for some genes categorized as lacking complementarity (Figures 2E, 2F, 3E, 5B, 5D, and 6C). These changes could be due to indirect effects. Alternatively, since most of these genes contain at least 7 nt of complementarity to the tRNA^{Leu} intron (Figure S3E), the required miRNA seed sequence length,⁵⁴ these effects could be mediated by latent short stretches of complementarity that are extended when accounting for mismatches. It is also plausible that fitRNAs function as RNA aptamers in a complementarity-independent fashion.^{35,55} fitRNA pull-down experiments will be critical to identify RNA/protein binding partners and elucidate mechanisms of fitRNA action.

The typical mechanism of miRNA-mediated decreases in mRNA levels requires loading of a Dicer-processed small RNA onto AGO proteins to form a complex that is guided to the 3' UTR of complementarity-bearing mRNA targets for cleavage and decay.⁵⁶ This pathway is even used in the context of some tRFs. For example, human pre-tRNA^{Leu} shifts from the classical cloverleaf to a long hairpin structure, which is a substrate for Dicer. The tRF-1 that is generated binds AGO proteins to mediate gene silencing.⁵⁷ However, since the *S. cerevisiae* genome lacks Dicer and AGO genes,⁵⁸ fitRNAs must function by an alternative mechanism(s).

The binding of fitRNAs to mRNAs may either be unassisted or aided by a currently unknown protein(s). Indeed, tRFs can bind target mRNAs through sequence complementarity, independent of AGO proteins, leading to disruption of target mRNA secondary

structure and subsequent translational repression.^{59,60} A protein-unassisted mechanism would also be supported by the hypothesis that noncanonical sncRNAs generated from longer RNAs (e.g., tRFs) evolved prior to the emergence of a more specialized form of RNA interference (RNAi) mediated by miRNAs, small interfering RNAs (siRNAs), and Piwi-interacting RNAs (piRNAs).³⁵ In support of this postulate, sncRNAs (including tRFs) are found in ancient unicellular organisms that lack miRNAs, siRNAs, and piRNAs, as well as Dicer³³ and are typically generated by ancient RNases such as RNase P and RNase Z. Furthermore, noncanonical sncRNAs are much more versatile, having many AGO-independent aptamer-like functions.³⁴ Given that fitRNAs are generated by the highly conserved SEN complex and are functional in the RNAi-deficient *S. cerevisiae*, fitRNAs may have evolved as an early form of RNAi.

Role of fitRNAs in stress response

In response to oxidative stress, fitRNA^{Trp} greatly accumulated, resulting in decreased levels of complementary mRNAs (Figure 6). This fitRNA build-up is mediated primarily by decreased fitRNA turnover, as new primary transcript production for all intron-containing tRNA families detected is rapidly shut down upon exposure to H₂O₂ (Figure S9B). We infer that multiple pathways for fitRNA turnover likely exist, since only some families of fitRNAs accumulate in response to H₂O₂, and even then, to differing extents (Figure 6B).

Like fitRNAs, mRNA introns and other classes of tRFs accumulate or are generated in response to cellular stress.^{35,61} For example, mRNA introns in yeast are typically rapidly degraded but accumulate under starvation conditions.⁶² These introns sequester the spliceosome and subsequently repress ribosomal protein gene expression as an adaptive response to starvation.^{62,63} Since none of the genes bearing complementarity to the tRNA^{Trp} intron are oxidative stress-related genes, the role of fitRNA^{Trp} in the cellular oxidative stress response remains to be determined.

Limitations of the study

The inducible tRNA^{Leu} intron overexpression system was useful in identifying specific and direct effects of fitRNAs on gene regulation. However, unlike endogenous tRNA introns that are generated by precise endonucleolytic cleavage of precursor tRNAs at the mitochondrial surface, this intron is nuclearly transcribed with 5' and 3' extensions. Although it moves to the cytoplasm with time (Figure S6D), interpretation of the mechanism(s) of fitRNA-mediated mRNA decay and the resulting biological consequences will benefit from the development of new methodologies that produce more endogenous-like fitRNAs. Furthermore, identification of the full range of fitRNA targets will be needed to determine the global cellular impact of fitRNAs under basal and stress conditions.

RESOURCE AVAILABILITY

Lead contact

Further information and requests for resources and reagents should be directed to and will be fulfilled by the lead contact, Anita K. Hopper (hopper.64@osu.edu).

Materials availability

Requests for plasmids or other resources generated in this study should be directed to and will be fulfilled by the [lead contact](#), Anita K. Hopper (hopper.64@osu.edu).

Data and code availability

- All data reported in this paper will be shared by the [lead contact](#) upon request.
- All original code is available at <https://github.com/hopper-aklab/tRNAintronsFunctionAsRegulatoryRNAs> and is deposited at Zenodo (<https://doi.org/10.5281/zenodo.14538031>) and is publicly available as of the date of publication.
- Any additional information required to reanalyze the data reported in this paper is available from the [lead contact](#) upon request.

ACKNOWLEDGMENTS

We are grateful to Dr. Venkat Gopalan and Dr. Guramrit Singh for their critical review of the manuscript, to Dr. Ralf Bundschuh and Jackson Hastings for assistance with the bioinformatics, to Dr. Hal S. Alper for kindly providing plasmids, to Dr. Paul K. Herman for providing use of the NanoDrop, to the Ohio Supercomputer Center for consultation, and the members of the A.K. Hopper lab for helpful scientific discussions and comments on the manuscript. We thank the Genomics Shared Resource at The Ohio State University Comprehensive Cancer Center, Columbus, OH for their Sanger sequencing services and acknowledge the allocation of computation resources from the Ohio Supercomputer Center. This work was supported by funding from the National Institutes of Health, grant number GM122884 to A.K.H.; Pelotonia undergraduate

fellowships to P.L.S., A.B., and L.M.P.; and Undergraduate Research Scholarship (URS) award to P.L.S.

AUTHOR CONTRIBUTIONS

Conceptualization, R.T.N., P.L.S., A.B., and A.K.H.; investigation, R.T.N., P.L.S., A.B., S.M., and L.M.P.; writing, R.T.N., P.L.S., S.M., and A.K.H.; supervision, A.K.H.

DECLARATION OF INTERESTS

A.K.H. is a member of the scientific advisory board of Zhuhai Codone Biotech. Co., Ltd.

STAR METHODS

Detailed methods are provided in the online version of this paper and include the following:

- [KEY RESOURCES TABLE](#)
- [EXPERIMENTAL MODEL AND STUDY PARTICIPANT DETAILS](#)
 - Yeast strains and growth and plasmids
 - tRNA^{Leu} intron deletion strains
- [METHOD DETAILS](#)
 - Bioinformatics
 - Small and total RNA isolation
 - Reverse transcription and qPCR
 - Tet-on system
 - Northern blot analysis
 - Western blot analysis
 - Yeast subcellular fractionation
- [QUANTIFICATION AND STATISTICAL ANALYSIS](#)

SUPPLEMENTAL INFORMATION

Supplemental information can be found online at <https://doi.org/10.1016/j.molcel.2025.01.019>.

Received: June 7, 2024

Revised: October 21, 2024

Accepted: January 17, 2025

Published: February 11, 2025

REFERENCES

1. Su, Z., Wilson, B., Kumar, P., and Dutta, A. (2020). Noncanonical roles of tRNAs: tRNA fragments and beyond. *Annu. Rev. Genet.* 54, 47–69. <https://doi.org/10.1146/annurev-genet-022620-101840>.
2. Schimmel, P. (2018). The emerging complexity of the tRNA world: mammalian tRNAs beyond protein synthesis. *Nat. Rev. Mol. Cell Biol.* 19, 45–58. <https://doi.org/10.1038/nrm.2017.77>.
3. Kim, H.K., Yeom, J.H., and Kay, M.A. (2020). Transfer RNA-derived small RNAs: another layer of gene regulation and novel targets for disease therapeutics. *Mol. Ther.* 28, 2340–2357. <https://doi.org/10.1016/j.mtthe.2020.09.013>.
4. Orellana, E.A., Siegal, E., and Gregory, R.I. (2022). tRNA dysregulation and disease. *Nat. Rev. Genet.* 23, 651–664. <https://doi.org/10.1038/s41576-022-00501-9>.
5. Phizicky, E.M., and Hopper, A.K. (2023). The life and times of a tRNA. *RNA* 29, 898–957. <https://doi.org/10.1261/rna.079620.123>.
6. Wu, J., Bao, A., Chatterjee, K., Wan, Y., and Hopper, A.K. (2015). Genome-wide screen uncovers novel pathways for tRNA processing and nuclear-cytoplasmic dynamics. *Genes Dev.* 29, 2633–2644. <https://doi.org/10.1101/gad.269803.115>.

7. Lee, M.C., and Knapp, G. (1985). Transfer RNA splicing in *Saccharomyces cerevisiae*. Secondary and tertiary structures of the substrates. *J. Biol. Chem.* **260**, 3108–3115.
8. Swerdlow, H., and Guthrie, C. (1984). Structure of intron-containing tRNA precursors. Analysis of solution conformation using chemical and enzymatic probes. *J. Biol. Chem.* **259**, 5197–5207.
9. Hayne, C.K., Lewis, T.A., and Stanley, R.E. (2022). Recent insights into the structure, function, and regulation of the eukaryotic transfer RNA splicing endonuclease complex. *Wiley Interdiscip. Rev. RNA* **13**, e1717. <https://doi.org/10.1002/wrna.1717>.
10. Sekulovski, S., Sušac, L., Stelz, L.S., Tampé, R., and Trowitzsch, S. (2023). Structural basis of substrate recognition by human tRNA splicing endonuclease TSEN. *Nat. Struct. Mol. Biol.* **30**, 834–840. <https://doi.org/10.1038/s41594-023-00992-y>.
11. Zhang, X., Yang, F., Zhan, X., Bian, T., Xing, Z., Lu, Y., and Shi, Y. (2023). Structural basis of pre-tRNA intron removal by human tRNA splicing endonuclease. *Mol. Cell* **83**, 1328–1339.e4. <https://doi.org/10.1016/j.molcel.2023.03.015>.
12. Hayne, C.K., Butay, K.J.U., Stewart, Z.D., Krahn, J.M., Perera, L., Williams, J.G., Petrovitch, R.M., Deterding, L.J., Matera, A.G., Borgnia, M.J., et al. (2023). Structural basis for pre-tRNA recognition and processing by the human tRNA splicing endonuclease complex. *Nat. Struct. Mol. Biol.* **30**, 824–833. <https://doi.org/10.1038/s41594-023-00991-z>.
13. Chan, P.P., and Lowe, T.M. (2016). GtRNAdb 2.0: an expanded database of transfer RNA genes identified in complete and draft genomes. *Nucleic Acids Res.* **44**, D184–D189. <https://doi.org/10.1093/nar/gkv1309>.
14. Haugen, P., Simon, D.M., and Bhattacharya, D. (2005). The natural history of group I introns. *Trends Genet.* **21**, 111–119. <https://doi.org/10.1016/j.tig.2004.12.007>.
15. Reinhold-Hurek, B., and Shub, D.A. (1992). Self-splicing introns in tRNA genes of widely divergent bacteria. *Nature* **357**, 173–176. <https://doi.org/10.1038/357173a0>.
16. Paushkin, S.V., Patel, M., Furia, B.S., Peltz, S.W., and Trotta, C.R. (2004). Identification of a human endonuclease complex reveals a link between tRNA splicing and pre-mRNA 3' end formation. *Cell* **117**, 311–321. [https://doi.org/10.1016/s0092-8674\(04\)00342-3](https://doi.org/10.1016/s0092-8674(04)00342-3).
17. Trotta, C.R., Miao, F., Arn, E.A., Stevens, S.W., Ho, C.K., Rauhut, R., and Abelson, J.N. (1997). The yeast tRNA splicing endonuclease: a tetrameric enzyme with two active site subunits homologous to the archaeal tRNA endonucleases. *Cell* **89**, 849–858. [https://doi.org/10.1016/s0092-8674\(00\)80270-6](https://doi.org/10.1016/s0092-8674(00)80270-6).
18. De Robertis, E.M., Black, P., and Nishikura, K. (1981). Intranuclear location of the tRNA splicing enzymes. *Cell* **23**, 89–93. [https://doi.org/10.1016/0092-8674\(81\)90273-7](https://doi.org/10.1016/0092-8674(81)90273-7).
19. Melton, D.A., De Robertis, E.M., and Cortese, R. (1980). Order and intracellular location of the events involved in the maturation of a spliced tRNA. *Nature* **284**, 143–148. <https://doi.org/10.1038/284143a0>.
20. Wan, Y., and Hopper, A.K. (2018). From powerhouse to processing plant: conserved roles of mitochondrial outer membrane proteins in tRNA splicing. *Genes Dev.* **32**, 1309–1314. <https://doi.org/10.1101/gad.316257.118>.
21. Yoshihisa, T., Yunoki-Esaki, K., Ohshima, C., Tanaka, N., and Endo, T. (2003). Possibility of cytoplasmic pre-tRNA splicing: the yeast tRNA splicing endonuclease mainly localizes on the mitochondria. *Mol. Biol. Cell* **14**, 3266–3279. <https://doi.org/10.1091/mbc.e02-11-0757>.
22. Knapp, G., Ogden, R.C., Peebles, C.L., and Abelson, J. (1979). Splicing of yeast tRNA precursors: structure of the reaction intermediates. *Cell* **18**, 37–45. [https://doi.org/10.1016/0092-8674\(79\)90351-9](https://doi.org/10.1016/0092-8674(79)90351-9).
23. Wu, J., and Hopper, A.K. (2014). Healing for destruction: tRNA intron degradation in yeast is a two-step cytoplasmic process catalyzed by tRNA ligase Rlg1 and 5'-to-3' exonuclease Xrn1. *Genes Dev.* **28**, 1556–1561. <https://doi.org/10.1101/gad.244673.114>.
24. Lu, Z., Filonov, G.S., Noto, J.J., Schmidt, C.A., Hatkevich, T.L., Wen, Y., Jaffrey, S.R., and Matera, A.G. (2015). Metazoan tRNA introns generate stable circular RNAs in vivo. *RNA* **21**, 1554–1565. <https://doi.org/10.1261/rna.052944.115>.
25. Salgia, S.R., Singh, S.K., Gurha, P., and Gupta, R. (2003). Two reactions of *Haloferax volcanii* RNA splicing enzymes: joining of exons and circularization of introns. *RNA* **9**, 319–330. <https://doi.org/10.1261/rna.2118203>.
26. Schmidt, C.A., and Matera, A.G. (2020). tRNA introns: presence, processing, and purpose. *Wiley Interdiscip. Rev. RNA* **11**, e1583. <https://doi.org/10.1002/wrna.1583>.
27. Hayashi, S., Mori, S., Suzuki, T., Suzuki, T., and Yoshihisa, T. (2019). Impact of intron removal from tRNA genes on *Saccharomyces cerevisiae*. *Nucleic Acids Res.* **47**, 5936–5949. <https://doi.org/10.1093/nar/gkz270>.
28. Ho, C.K., and Abelson, J. (1988). Testing for intron function in the essential *Saccharomyces cerevisiae* tRNA(SerUCG) gene. *J. Mol. Biol.* **202**, 667–672. [https://doi.org/10.1016/0022-2836\(88\)90295-1](https://doi.org/10.1016/0022-2836(88)90295-1).
29. Donze, D., and Kamakaka, R.T. (2001). RNA polymerase III and RNA polymerase II promoter complexes are heterochromatin barriers in *Saccharomyces cerevisiae*. *EMBO J.* **20**, 520–531. <https://doi.org/10.1093/emboj/20.3.520>.
30. Randau, L., and Söll, D. (2008). Transfer RNA genes in pieces. *EMBO Rep.* **9**, 623–628. <https://doi.org/10.1038/embor.2008.101>.
31. Payea, M.J., Hauke, A.C., De Zoysa, T., and Phizicky, E.M. (2020). Mutations in the anticodon stem of tRNA cause accumulation and Met22-dependent decay of pre-tRNA in yeast. *RNA* **26**, 29–43. <https://doi.org/10.1261/rna.073155.119>.
32. Grosjean, H., Szwejkowska-Kulinska, Z., Motorin, Y., Fasiolo, F., and Simos, G. (1997). Intron-dependent enzymatic formation of modified nucleosides in eukaryotic tRNAs: a review. *Biochimie* **79**, 293–302. [https://doi.org/10.1016/s0300-9084\(97\)83517-1](https://doi.org/10.1016/s0300-9084(97)83517-1).
33. Shabalina, S.A., and Koonin, E.V. (2008). Origins and evolution of eukaryotic RNA interference. *Trends Ecol. Evol.* **23**, 578–587. <https://doi.org/10.1016/j.tree.2008.06.005>.
34. Chen, Q., Zhang, X., Shi, J., Yan, M., and Zhou, T. (2021). Origins and evolving functionalities of tRNA-derived small RNAs. *Trends Biochem. Sci.* **46**, 790–804. <https://doi.org/10.1016/j.tibs.2021.05.001>.
35. Chen, Q., and Zhou, T. (2023). Emerging functional principles of tRNA-derived small RNAs and other regulatory small RNAs. *J. Biol. Chem.* **299**, 105225. <https://doi.org/10.1016/j.jbc.2023.105225>.
36. Yu, X., Xie, Y., Zhang, S., Song, X., Xiao, B., and Yan, Z. (2021). tRNA-derived fragments: mechanisms underlying their regulation of gene expression and potential applications as therapeutic targets in cancers and virus infections. *Theranostics* **11**, 461–469. <https://doi.org/10.7150/thno.51963>.
37. Tuller, T., Ruppin, E., and Kupiec, M. (2009). Properties of untranslated regions of the *S. cerevisiae* genome. *BMC Genomics* **10**, 391. <https://doi.org/10.1186/1471-2164-10-391>.
38. Kramer, E.B., and Hopper, A.K. (2013). Retrograde transfer RNA nuclear import provides a new level of tRNA quality control in *Saccharomyces cerevisiae*. *Proc. Natl. Acad. Sci. USA* **110**, 21042–21047. <https://doi.org/10.1073/pnas.1316579110>.
39. Gu, S., and Kay, M.A. (2010). How do miRNAs mediate translational repression? *Silence* **1**, 11. <https://doi.org/10.1186/1758-907X-1-11>.
40. Imburgio, D., Rong, M., Ma, K., and McAllister, W.T. (2000). Studies of promoter recognition and start site selection by T7 RNA polymerase using a comprehensive collection of promoter variants. *Biochemistry* **39**, 10419–10430. <https://doi.org/10.1021/bi000365w>.
41. Davidson, E.A., Van Blarcom, T., Levy, M., and Ellington, A.D. (2010). Emulsion based selection of T7 promoters of varying activity. In Pacific Symposium on Biocomputing, pp. 433–443. https://doi.org/10.1142/9789814295291_0045.
42. McAllister, W.T., Morris, C., Rosenberg, A.H., and Studier, F.W. (1981). Utilization of bacteriophage T7 late promoters in recombinant plasmids

- during infection. *J. Mol. Biol.* 153, 527–544. [https://doi.org/10.1016/0022-2836\(81\)90406-x](https://doi.org/10.1016/0022-2836(81)90406-x).
43. Tabor, S., and Richardson, C.C. (1985). A bacteriophage T7 RNA polymerase/promoter system for controlled exclusive expression of specific genes. *Proc. Natl. Acad. Sci. USA* 82, 1074–1078. <https://doi.org/10.1073/pnas.82.4.1074>.
44. Timney, B.L., Raveh, B., Mironská, R., Trivedi, J.M., Kim, S.J., Russel, D., Wente, S.R., Sali, A., and Rout, M.P. (2016). Simple rules for passive diffusion through the nuclear pore complex. *J. Cell Biol.* 215, 57–76. <https://doi.org/10.1083/jcb.201601004>.
45. Garneau, N.L., Wilusz, J., and Wilusz, C.J. (2007). The highways and byways of mRNA decay. *Nat. Rev. Mol. Cell Biol.* 8, 113–126. <https://doi.org/10.1038/nrm2104>.
46. Kilchert, C., Wittmann, S., and Vasiljeva, L. (2016). The regulation and functions of the nuclear RNA exosome complex. *Nat. Rev. Mol. Cell Biol.* 17, 227–239. <https://doi.org/10.1038/nrm.2015.15>.
47. Araki, Y., Takahashi, S., Kobayashi, T., Kajiho, H., Hoshino, S., and Katada, T. (2001). Ski7p G protein interacts with the exosome and the Ski complex for 3'-to-5' mRNA decay in yeast. *EMBO J.* 20, 4684–4693. <https://doi.org/10.1093/emboj/20.17.4684>.
48. Nostramo, R.T., and Hopper, A.K. (2020). A novel assay provides insight into tRNAPhe retrograde nuclear import and re-export in *S. cerevisiae*. *Nucleic Acids Res.* 48, 11577–11588. <https://doi.org/10.1093/nar/gkaa879>.
49. Chatterjee, K., Marshall, W.A., and Hopper, A.K. (2022). Three tRNA nuclear exporters in *S. cerevisiae*: parallel pathways, preferences, and precision. *Nucleic Acids Res.* 50, 10140–10152. <https://doi.org/10.1093/nar/gkac754>.
50. Murthi, A., Shaheen, H.H., Huang, H.Y., Preston, M.A., Lai, T.P., Phizicky, E.M., and Hopper, A.K. (2010). Regulation of tRNA bidirectional nuclear–cytoplasmic trafficking in *Saccharomyces cerevisiae*. *Mol. Biol. Cell* 21, 639–649. <https://doi.org/10.1091/mbc.E09-07-0551>.
51. Shaheen, H.H., and Hopper, A.K. (2005). Retrograde movement of tRNAs from the cytoplasm to the nucleus in *Saccharomyces cerevisiae*. *Proc. Natl. Acad. Sci. USA* 102, 11290–11295. <https://doi.org/10.1073/pnas.0503836102>.
52. Kufel, J., and Tollervey, D. (2003). 3'-processing of yeast tRNATrp precedes 5'-processing. *RNA* 9, 202–208. <https://doi.org/10.1261/rna.2145103>.
53. Cavalier-Smith, T. (1991). Intron phylogeny: a new hypothesis. *Trends Genet.* 7, 145–148.
54. Bartel, D.P. (2009). MicroRNAs: target recognition and regulatory functions. *Cell* 136, 215–233. <https://doi.org/10.1016/j.cell.2009.01.002>.
55. Ying, S., Li, P., Wang, J., Chen, K., Zou, Y., Dai, M., Xu, K., Feng, G., Zhang, C., Jiang, H., et al. (2023). tRF-Gln-CTG-026 ameliorates liver injury by alleviating global protein synthesis. *Signal Transduct. Target. Ther.* 8, 144. <https://doi.org/10.1038/s41392-023-01351-5>.
56. Ghildiyal, M., and Zamore, P.D. (2009). Small silencing RNAs: an expanding universe. *Nat. Rev. Genet.* 10, 94–108. <https://doi.org/10.1038/nrg2504>.
57. Hasler, D., Lehmann, G., Murakawa, Y., Klironomos, F., Jakob, L., Grässer, F.A., Rajewsky, N., Landthaler, M., and Meister, G. (2016). The lupus autoantigen la prevents mis-channeling of tRNA fragments into the human microRNA pathway. *Mol. Cell* 63, 110–124. <https://doi.org/10.1016/j.molcel.2016.05.026>.
58. Drinnenberg, I.A., Weinberg, D.E., Xie, K.T., Mower, J.P., Wolfe, K.H., Fink, G.R., and Bartel, D.P. (2009). RNAi in budding yeast. *Science* 326, 544–550. <https://doi.org/10.1126/science.1176945>.
59. Kim, H.K., Xu, J., Chu, K., Park, H., Jang, H., Li, P., Valdmanis, P.N., Zhang, Q.C., and Kay, M.A. (2019). A tRNA-derived small RNA regulates ribosomal protein S28 protein levels after translation initiation in humans and mice. *Cell Rep.* 29, 3816–3824.e4. <https://doi.org/10.1016/j.celrep.2019.11.062>.
60. Kim, H.K., Fuchs, G., Wang, S., Wei, W., Zhang, Y., Park, H., Roy-Chaudhuri, B., Li, P., Xu, J., Chu, K., et al. (2017). A transfer-RNA-derived small RNA regulates ribosome biogenesis. *Nature* 552, 57–62. <https://doi.org/10.1038/nature25005>.
61. Saikia, M., and Hatzoglou, M. (2015). The many virtues of tRNA-derived stress-induced RNAs (tiRNAs): discovering novel mechanisms of stress response and effect on human health. *J. Biol. Chem.* 290, 29761–29768. <https://doi.org/10.1074/jbc.R115.694661>.
62. Morgan, J.T., Fink, G.R., and Bartel, D.P. (2019). Excised linear introns regulate growth in yeast. *Nature* 565, 606–611. <https://doi.org/10.1038/s41586-018-0828-1>.
63. Parenteau, J., Maignon, L., Berthoumieux, M., Catala, M., Gagnon, V., and Abou Elela, S. (2019). Introns are mediators of cell response to starvation. *Nature* 565, 612–617. <https://doi.org/10.1038/s41586-018-0859-7>.
64. Davis, L.I., and Fink, G.R. (1990). The NUP1 gene encodes an essential component of the yeast nuclear pore complex. *Cell* 61, 965–978. [https://doi.org/10.1016/0092-8674\(90\)90062-j](https://doi.org/10.1016/0092-8674(90)90062-j).
65. Maccecchini, M.L., Rudin, Y., Blobel, G., and Schatz, G. (1979). Import of proteins into mitochondria: precursor forms of the extramitochondrially made F1-ATPase subunits in yeast. *Proc. Natl. Acad. Sci. USA* 76, 343–347. <https://doi.org/10.1073/pnas.76.1.343>.
66. Hopper, A.K., Traglia, H.M., and Dunst, R.W. (1990). The yeast RNA1 gene product necessary for RNA processing is located in the cytosol and apparently excluded from the nucleus. *J. Cell Biol.* 111, 309–321. <https://doi.org/10.1083/jcb.111.2.309>.
67. Li, Z., Vizeacoumar, F.J., Bahr, S., Li, J., Warringer, J., Vizeacoumar, F.S., Min, R., Vandersluys, B., Bellay, J., Devit, M., et al. (2011). Systematic exploration of essential yeast gene function with temperature-sensitive mutants. *Nat. Biotechnol.* 29, 361–367. <https://doi.org/10.1038/nbt.1832>.
68. Morse, N.J., Wagner, J.M., Reed, K.B., Gopal, M.R., Lauffer, L.H., and Alper, H.S. (2018). T7 polymerase expression of guide RNAs in vivo allows exportable CRISPR-Cas9 editing in multiple yeast hosts. *ACS Synth. Biol.* 7, 1075–1084. <https://doi.org/10.1021/acssynbio.7b00461>.
69. Roney, I.J., Rudner, A.D., Couture, J.F., and Kærn, M. (2016). Improvement of the reverse tetracycline transactivator by single amino acid substitutions that reduce leaky target gene expression to undetectable levels. *Sci. Rep.* 6, 27697. <https://doi.org/10.1038/srep27697>.
70. Horecka, J., and Davis, R.W. (2014). The 50:50 method for PCR-based seamless genome editing in yeast. *Yeast* 31, 103–112. <https://doi.org/10.1002/yea.2992>.
71. Gietz, R.D., and Schiestl, R.H. (2007). High-efficiency yeast transformation using the LiAc/SS carrier DNA/PEG method. *Nat. Protoc.* 2, 31–34. <https://doi.org/10.1038/nprot.2007.13>.
72. Wong, E.D., Miyasato, S.R., Aleksander, S., Karra, K., Nash, R.S., Skrzypek, M.S., Weng, S., Engel, S.R., and Cherry, J.M. (2023). *Saccharomyces* genome database update: server architecture, pan-genome nomenclature, and external resources. *Genetics* 224, iyac191. <https://doi.org/10.1093/genetics/iyac191>.
73. Engel, S.R., Wong, E.D., Nash, R.S., Aleksander, S., Alexander, M., Douglass, E., Karra, K., Miyasato, S.R., Simison, M., Skrzypek, M.S., et al. (2022). New data and collaborations at the *Saccharomyces* Genome Database: updated reference genome, alleles, and the Alliance of Genome Resources. *Genetics* 220, iyab224. <https://doi.org/10.1093/genetics/iyab224>.
74. Pelechano, V., Wei, W., and Steinmetz, L.M. (2013). Extensive transcriptional heterogeneity revealed by isoform profiling. *Nature* 497, 127–131. <https://doi.org/10.1038/nature12121>.

75. Shen, X.X., Opulente, D.A., Kominek, J., Zhou, X., Steenwyk, J.L., Buh, K.V., Haase, M.A.B., Wisecaver, J.H., Wang, M., Doering, D.T., et al. (2018). Tempo and mode of genome evolution in the budding yeast subphylum. *Cell* 175, 1533–1545.e20. <https://doi.org/10.1016/j.cell.2018.10.023>.
76. Lemoine, F., Correia, D., Lefort, V., Doppelt-Azeroual, O., Mareuil, F., Cohen-Boulakia, S., and Gascuel, O. (2019). NGPhylogeny.fr: new generation phylogenetic services for non-specialists. *Nucleic Acids Res.* 47, W260–W265. <https://doi.org/10.1093/nar/gkz303>.
77. Calvopina-Chavez, D.G., Gardner, M.A., and Griffitts, J.S. (2022). Engineering efficient termination of bacteriophage T7 RNA polymerase transcription. *G3 (Bethesda)* 12, jkac070. <https://doi.org/10.1093/g3journal/jkac070>.
78. Wu, J., Huang, H.Y., and Hopper, A.K. (2013). A rapid and sensitive non-radioactive method applicable for genome-wide analysis of *Saccharomyces cerevisiae* genes involved in small RNA biology. *Yeast* 30, 119–128. <https://doi.org/10.1002/yea.2947>.
79. Neumann, H., Bartle, L., Bonnell, E., and Wellinger, R.J. (2023). Ratcheted transport and sequential assembly of the yeast telomerase RNP. *Cell Rep.* 42, 113565. <https://doi.org/10.1016/j.celrep.2023.113565>.

STAR★METHODS

KEY RESOURCES TABLE

REAGENT or RESOURCE	SOURCE	IDENTIFIER
Antibodies		
6x-His Tag Monoclonal Antibody (HIS.H8)	Invitrogen	Cat# MA1-21315; RRID: AB_557403
Mouse Monoclonal Antibody to Nsp1p	EnCor Biotech	Cat# MCA-32D6; RRID: AB_2157646
Anti-Ran antibody ab4781 also named Gsp1	Abcam	N/A
IRDye® 800CW Goat anti-Rabbit IgG Secondary Antibody	LI-CORbio	RRID: AB_2651127
IRDye® 680RD Goat anti-Mouse IgG Secondary Antibody	LI-CORbio	RRID: AB_2651128
Mouse anti-Nup1	Gift from Davis and Fink ⁶⁴	N/A
Rabbit anti-Atp2, originally from the G. Schatz lab	Gift from M Yaffe ⁶⁵	N/A
Rabbit anti-Rna1	Hopper et al. ⁶⁶	N/A
Experimental models: Organisms/strains		
<i>Saccharomyces cerevisiae</i> BY4741	ATCC	ATCC 4040002
tRNA ^{lle} intron deletion strain (GN7-56)	This study	N/A
tRNA ^{lle} intron deletion strain with dual cassettes (GN4-14)	This study	N/A
tRNA ^{lle} intron control strain with dual cassettes (GN5-31)	This study	N/A
<i>tom70Δ, los1Δ, rrp6Δ, ski7Δ, xrn1Δ</i>	From the <i>S. cerevisiae</i> MATa deletion collection	https://horizondiscovery.com/en/non-mammalian-research-tools/products/yeast-knockout
<i>sen2-1, dis3-1, rat1-1</i>	From the Boone lab; Li et al. ⁶⁷	N/A
Oligonucleotides		
See Tables S4 and S7 and tRNAlle deletion strains construction in STAR Methods section experimental model and study participant details.	A.K. Hopper Lab & this study	N/A
Recombinant DNA		
tRNA ^{lle} -pRS416	This study	N/A
tRNA ^{lle} Δ -pRS416	This study	N/A
TDH3pro-rtTA-tetO7pro-T7pol-pRS413 (tet-on OE system, plasmid 1)	This study	N/A
T7pro-tRNA ^{ITSlle} intron-T7termVar1-pRS426 (tet-on OE system, plasmid 2)	This study	N/A
T7pro-tRNA ^{ITSlle} intron-T7term-pRS426	This study	N/A
T7pro-tRNA ^{GG-lle} intron-T7term-prs426	This study	N/A
T7pro-tRNA ^{lle} intron-T7term-pRS426	This study	N/A
T7pro-tRNA ^{ITSlle} intron-T7term _{Hyb6} -pRS426	This study	N/A
T7pro-tRNA ^{ITSlle} intron-T7term _{Var2} -pRS426	This study	N/A
T7pro-tRNA ^{ITSlle} intron-T7term _{Var3} -pRS426	This study	N/A
p413-TEF-T7Pro-sgRNA-T7pol-LeuInt	Morse et al. ⁶⁸	N/A
TDH3pro-rtTA-M2-SE-G72P	Roney et al. ⁶⁹	Addgene #177924
Gpm2-6xHIS-pRS416	This study	N/A
tRNA ^{lle} -1-3' Exon-75nt term-KanMX6-pRS416	This study	N/A
tRNA ^{lle} -2-3' Exon-75nt term-His3MX6-pRS416	This study	N/A

(Continued on next page)

Continued

REAGENT or RESOURCE	SOURCE	IDENTIFIER
tRNA ^{ITS-Ile(M25-33)} -pRS426	This study	N/A
tRNA ^{ITS-Ile(M30-38)} -pRS426	This study	N/A
Software and algorithms		
ImageJ	National Institutes of Health	https://imagej.nih.gov/ij/
GraphPad Prism 9	GraphPad Software	https://www.graphpad.com/scientific-software/prism/www.graphpad.com/scientific-software/prism/
LI-COR Image Studio	LI-COR Bio	https://www.licor.com/bio/image-studio/
Gene ontology analysis was performed using the Gene Ontology feature in the <i>Saccharomyces</i> genome database	Stanford University	https://www.yeastgenome.org/
Other		
Computational analyses were performed using custom Python programs	This study	https://github.com/hopper-aklab/tRNAsIntronFunctionAsRegulatoryRNAs; deposited at Zenodo (https://doi.org/10.5281/zenodo.14538031; DOI: https://doi.org/10.5281/zenodo.14538031)
The <i>S. cerevisiae</i> coding genome and UTR sequences were sourced from the <i>Saccharomyces</i> genome database	Stanford University	https://www.yeastgenome.org/
The human coding genome was sourced from the NCBI human genome resource (GRCh38)	NCBI	https://www.ncbi.nlm.nih.gov/genome/guide/human/

EXPERIMENTAL MODEL AND STUDY PARTICIPANT DETAILS

Yeast strains and growth and plasmids

All *S. cerevisiae* strains used in this study were derived from BY4741 (*MATA his3Δ leu2Δ met15Δ ura3Δ*). The *sen2-1*, *rat1-1* and *dis3-1* strains were provided by the Boone lab.⁶⁷ The *tom70Δ*, *los1Δ*, *rrp6Δ*, *ski7Δ* and *xrn1Δ* strains were from the yeast deletion collection. The tRNA^{Ile} intron deletion strain was generated using the 50:50 method for seamless deletion.⁷⁰ The tRNA^{ITS-Ile} intron mutant plasmids were made by PCR-based site directed mutagenesis. Yeast strains were grown at 23°C in either yeast extract with peptone media supplemented with 2% glucose (YEPD) or synthetic complete media supplemented with 2% glucose (SCD) for cells expressing plasmids with prototrophic markers. For temperature sensitive mutants, cultures were shifted to 37°C for the time indicated. For H₂O₂ experiments, 0.5-3mM H₂O₂ was added to YEPD cultures for <1 min to 2h. Yeast strains and plasmids used in this study are described in Tables S5 and S6.

tRNA^{Ile} intron deletion strains

The seamless tRNA^{Ile} intron deletion strain was generated using the 50:50 method for seamless yeast genome editing as described by Horecka and Davis.⁷⁰ The forward primers used for deletion of the tRNA^{Ile-1} and tRNA^{Ile-2} introns (listed 5' to 3') were:

TCGAAAATGCTCGTGTAGCTCAGTGGTTAGAGCTCGTGCTTAAACGCGACCGTCTGGGTTCAAACCCCACCTCGAG-
CACTTTCTCTTTTTTACACCGTACGCTGCAGGTCGAC (Forward for tRNA^{Ile-1})

TCGAAAATGCTCGTGTAGCTCAGTGGTTAGAGCTCGTGCTTAAACGCGACCGTCTGGGTTCAAACCCCACCTCGAG-
CACTTTCTCTTTTTAAACGTACGCTGCAGGTCGAC (Forward for tRNA^{Ile-2})

The same reverse primer was used for both tRNA^{Ile} genes (listed 5' to 3'): GGCCTGTTGAAAGGTCTTGGCACA
GAAACTTCGGAACCGAATGTTGCATCGATGAATTGAGCTCG.

Additionally, a second tRNA^{Ile} intron deletion strain was generated that contains the KanMX6 cassette or the His3MX6 cassette between nucleotides 75 and 76 downstream of the tRNA^{Ile-1} and tRNA^{Ile-2} genes, respectively. This dual cassette-containing strain was generated by first making a pRS416 plasmid containing the KanMX6 or His3MX6 cassettes inserted between Xmal and Xbal sites. Then the 3' exon of tRNA^{Ile-1} or tRNA^{Ile-2} + 75bp of terminator sequence was inserted into the pRS416-KanMX6 or pRS416-His3MX6 plasmids, respectively, using Xhol and Xmal restriction sites. To generate the cassette-containing tRNA^{Ile} intron deletion strain, these plasmids were PCR amplified using F primers that contained the sequence upstream of the 5' exon, the entire 5' exon and the beginning of the 3' exon. The reverse primer contained the first 75-nts of the terminator sequence and the KanMX6 or HisMX6 cassette terminator sequence. The PCR product was run on a 1% agarose gel, gel purified and transformed into BY4741

yeast cells using the LiAc/SS carrier/DNA/PEG method.⁷¹ A control strain, containing the introns and the cassettes, was generated by the same approach, but using a F primer containing the sequence of the tRNA^{lle} intron and 3' exon. The primers used (listed 5' to 3') were as follows:

```
TTATTTACGTCTTTCGAAAATGCTCGTAGCTCAGTGGTAGAGCTCGTGCCTATAACGCGACCGTCGTGGTTCAA
(tRNAlle-1 intron deletion-F)
AATTGGTGATTTAACTCTTCGATTAATCTACTGAAAAAAAAAAAAAGAACCAAGTATAGCGACCAGCATT C (tRNAlle-
1 intron deletion-R)
TAATTTACGTCTTTCGAAAATGCTCGTAGCTCAGTGGTAGAGCTCGTGCCTATAACGCGACCGTCGTGGTTCAA
(tRNAlle-2 intron deletion-F)
GATGTTAGAACAAATGTGCCGTATTCACCTGTATATGTGGATTATCTAACAGTCTACACAGTATAGCGACCAGCATT C (tRNAlle-
2 intron deletion-R)
GCAACATTCCGTTCCGAAGTTCTGTGCCAAAGACCTTCAAACAGGCCTTAAAAGCAACGCGACCGTCGTGGTTCAA
(tRNAlle-1 and tRNAlle-2 control-F)
```

The dual cassette-containing tRNA^{lle} intron deletion strain and the dual cassette-containing, intron-containing control strain were used to confirm all results in **Figure 2**, which use the seamless tRNA^{lle} intron deletion strain. The results using the seamless tRNA^{lle} intron deletion strain and the cassette-bearing tRNA^{lle} intron deletion strain were similar.

METHOD DETAILS

Bioinformatics

Identification of complementary ORFs, and related computational analyses, were performed using custom-made Python programs. Complementary ORFs identified in *S. cerevisiae* were cross-checked using the Saccharomyces genome database (SGD) yeast genome pattern matching webtool.⁷² Mature tRNA and tRNA intron sequences were obtained from the genomic tRNA database (GtRNAdb).¹³ The *S. cerevisiae* coding genome and UTR sequences were sourced from the SGD.^{73,74} The stringent parameter of at least 13-nts perfect complementarity ($\geq 13/13$ -nts) or 15-nts allowing for a single mismatch ($\geq 14/15$ -nts) using standard Watson-Crick-Franklin base pairing rules was semi-arbitrarily selected, as it identifies genes bearing complementarity at levels that are statistically improbable and yields a reasonable number of genes that could be analyzed both as a group and individually. For analysis of genes with tRNA^{lle} intron complementarity located in the 3' UTR, to obtain a larger dataset, we lowered the criteria to $\geq 12/12$ -nts or $\geq 13/14$ -nts. For "intron scrambling" experiments (Figures 1C and 1F), <1% of data points exceed the depicted y-axis and are not displayed for visual clarity. Gene ontology terms were identified using the SGD biological process slim term mapper.⁷³ To identify tRNA intron complementarity in humans, coding ORFs from the NCBI human genome resource (GRCh38) were screened. For coding ORFs with multiple isoforms, complementarity in a single isoform was sufficient for our criteria. Code and documentation are available at <https://github.com/hopper-aklab/tRNAsFunctionAsRegulatoryRNAs> and are deposited at Zenodo (<https://doi.org/10.5281/zenodo.14538031>).

For tRNA sequence conservation analysis in closely related yeasts, tRNA intron sequences were obtained from the GtRNAdb or from the organisms' relevant NCBI database. Organisms with multiple differing intron sequences are classified by the chromosome that the tRNA genes are present on. If two are on the same chromosome, they are listed sequentially based on their position on the chromosome. Divergence times were obtained from Shen et al.⁷⁵ by locating the most recent shared node with *S. cerevisiae* for each species. Species that are not present in Shen et al., are listed as unavailable. Alignment was performed using MUSCLE on the NGPhylogeny.fr webserver.⁷⁶ Nucleotide identity was calculated using the Needleman-Wunsch Global Align NCBI webtool. Default algorithm parameters were used for all programs.

Small and total RNA isolation

Yeast cultures (~15mL) at an OD₆₀₀ of 0.2-0.6 were pelleted and resuspended in TSE buffer (10mM Tris-HCl pH. 7.4, 0.1M NaCl, 10mM EDTA pH 8.0). For small RNA isolation, as described previously,²⁰ cells were resuspended in 500µL TSE buffer. 500µL TSE-saturated phenol (pH 6.6) was added and samples were transferred to a 2mL microcentrifuge tube. Tubes were incubated at 55°C for 3min, then vortexed at 1150rpm for 30sec to mix. This incubation/vortex cycle was repeated a total of 6 times. Tubes were incubated on ice for 10min, then centrifuged at 15000g for 10min at 4°C. The supernatant was transferred to a new 2mL microcentrifuge tube containing 200µL TSE-saturated phenol (pH 6.6) and mixed by inverting. Tubes were centrifuged at the same conditions one more time. The supernatants were transferred to a 2mL microcentrifuge tube containing 1250µL ice-cold 100% ethanol. Tubes were stored at -80°C for at least 1h.

For total RNA isolation, cells were resuspended in 200µL TSE buffer and transferred to a glass test tube with an equal volume of acid-washed glass beads and placed on ice. Tubes were cover with parafilm and vortexed 3 times for 30sec each, with incubation on ice for at least 1min between each round of vortexing. 235µL TSE was added and cultures were vortexed for 15sec. The cell lysate was transferred to a 1.5mL microcentrifuge tube on ice. An additional 235µL TSE was added to the beads. The cultures were again vortexed for 15sec and the cell lysate added to the same microcentrifuge tube. 400µL TSE-saturated phenol (pH 4.3) was added to the cell lysate. The tubes were mixed by inverting and centrifuged at 15000g for 10min at 4°C. The supernatant was transferred to a second 1.5mL microcentrifuge tube containing cold 250µL TSE-saturated phenol (pH 4.3) and 250µL chloroform. The tubes were

inverted to mix and centrifuged for another 10min as above. The supernatant was transferred into a 1.5mL microcentrifuge tube containing cold 175 μ L TSE-saturated phenol (pH 4.3) and 175 μ L chloroform. After centrifuging at 15000g for 10min at 4°C, the supernatant was transferred to a new 1.5mL microcentrifuge tube containing 500 μ L isopropanol (1 volume) and 50 μ L 3M sodium acetate pH 5.2 (0.1 volume). Tubes were stored at -80°C for at least 1h.

To precipitate RNA for small or total RNA isolation, microcentrifuge tubes were centrifuged at 15000g for 20min at 4°C to pellet RNA. The supernatant was removed and the pellet was washed with 1mL cold 70% ethanol. Tubes were centrifuged at 15000g for 5min at 4°C. The supernatant was again removed and the cell pellet left to air dry at room temperature for 10-15min. The RNA was resuspended in 30-50 μ L DNase/RNase-free dH₂O. RNA concentrations were measured using the NanoDrop 2000C (kindly provided by Dr. Paul Herman, OSU).

Reverse transcription and qPCR

Following RNA isolation, 8000ng RNA was treated with DNase using the Turbo DNA-free kit. After DNase treatment, RNA concentrations were measured again, at least in duplicate, using the NanoDrop 2000C. Reverse transcription for poly(A) RNA and tRNA^{le} was performed using ~1500ng or ~400ng RNA, respectively, RevertAid Reverse Transcriptase, RiboLock RNase inhibitor and either an oligo(dT)15 primer, a tRNA^{le} intron reverse primer (IVY3), a tRNA^{ITS-le} intron reverse primer (GN1001), or a mature tRNA^{le} reverse primer (IVY149). Quantitative PCR was performed using the QuantStudio3 instrument and the PowerUp SYBR green master mix, using cDNA diluted 5x if using an oligo(dT) primer or 2x if using a mature tRNA^{le}, tRNA^{le} intron, or tRNA^{ITS-le} intron primer. RT-qPCR of WT and mutated forms of the tRNA^{ITS-le} intron was performed using a reverse primer complementary to the 8-nts of the 3' end of the tRNA^{le} intron plus the 14-nts of the 5' end of the T7 terminator sequence (Var1; **Figure S6C**) and a forward primer complementary to the 6-nt ITS sequence plus the first 12-nts at the 5' end of the tRNA^{le} intron.

RNA levels are normalized to total RNA and quantified using a standard curve. Technical duplicates or triplicates were performed for each biological replicate. Melting curve analysis was performed to ensure amplification of a single target. No template and no reverse transcriptase controls were performed for each experiment to confirm the absence of DNA contamination. Primers for qPCR are provided in **Table S4**.

Tet-on system

Cells were transformed with a yeast centromere plasmid (Plasmid 1, **Figure 3A**) containing the gene for the reverse tetracycline trans-activator (rtTA), modified to have high-sensitivity and low leakiness (rtTA-M2-SE-G72P) and under the control of the strong, constitutive TDH3 promoter (Addgene Plasmid # 177924).⁶⁹ This plasmid also contains a tetracycline-responsive element (TRE) followed by the CYC1 promoter controlling the expression of the T7 polymerase gene, modified to contain a SV40 nuclear localization signal (NLS) between amino acids 10-11 and to have reduced abortive transcription (P266L; analogous to P278L in the T7 polymerase containing the NLS). The T7 polymerase gene was derived from plasmid #11 (**Table S5**), kindly provided by H.S. Alper (University of Texas at Austin).⁶⁸

Upon treatment with doxycycline (DOX), a DOX-rtTA complex forms, altering the conformation of the rtTA and allowing its binding to the TRE. This results in RNA polymerase II-mediated transcription of the T7 polymerase gene. The newly expressed T7 polymerase localizes to the nucleus, where it binds to the T7 promoter of a second, 2-micron (high-copy) plasmid (Plasmid 2, **Figure 3A**). In this plasmid, the T7 promoter is followed by the tRNA^{le} intron sequence and a T7 terminator, both of which were modified to optimize intron expression. It should be noted that the pRS426 plasmid contains a T7 promoter upstream of the inserted T7 promoter. However, its presence had little impact on tRNA intron expression (data not shown).

It has been previously shown that the 5' addition of 2-3 guanosines (G) or the sequence GGGAGA, referred to as the initially transcribed sequence (ITS), improves expression of the gene downstream of the T7 promoter.^{40,41} Our results indicated that the addition of a 5' ITS sequence to the tRNA^{le} intron (tRNA^{ITS-le} intron) resulted in a greater than 5-fold increase in expression as compared to the endogenous or 5'-GG amended tRNA^{le} intron sequence (**Figure S6A**). Therefore, the tRNA^{ITS-le} intron was used in all tet-on over-expression experiments.

The T7 terminator was also modified. Since the T7 polymerase is highly-processive, it is prone to read-through transcription, resulting in RNAs that are longer than desired.^{42,43} Indeed, when the tRNA^{ITS-le} intron was followed by the endogenous 53-nt T7 terminator sequence, the resulting species was approximately double the length of the endogenous tRNA^{le} intron, as shown by northern blot (**Figures S6B** and S6C, WT). Altering the T7 terminator sequence to the T7t_{hyb6} terminator sequence⁷⁷ led to a shorter intron product, but was still much larger than the endogenous 60-nt tRNA^{le} intron (**Figures S6B** and S6C, Hyb6). We therefore made three additional T7 terminator sequence variants and assessed their effects on the tRNA^{ITS-le} intron size and expression (**Figure S6C**). T7 terminator variant 1 (T7t_{var1}) elicited a large DOX-induced increase in a tRNA^{ITS-le} intron that was much closer in size to the endogenous tRNA^{le} intron, as well as a more lowly-expressed intron species at a slightly larger size (**Figure S6B**, Var1). Therefore, we utilized the T7t_{var1} sequence for all further experiments.

Lastly, it should be noted that a two-plasmid (rather than a one-plasmid) system was optimal. The high-copy plasmid #2 allowed for enhanced tRNA^{ITS-le} expression, whereas the low copy plasmid #1 kept rtTA expression at levels that minimized leakiness.⁶⁹ See **Methods S1** for the sequences of plasmids 1 and 2.

Northern blot analysis

Northern blot analysis was performed as described in detail previously⁷⁸ using the probes listed in Table S7. 5S rRNA, detected by ethidium bromide staining, served as a loading control. Quantitation of northern blots was performed using ImageJ software.

The northern blots for Figures 6A and S9B were probed with an oligonucleotide complementary to a single tRNA intron family (oligo 1), stripped, then reprobed with an oligonucleotide complementary to a second tRNA intron family (oligo 2). The probing pairs and order was as follows: Blot A: tRNA^{Ile} (oligo 1), tRNA^{Phe} (oligo 2); Blot B: tRNA^{Trp} (oligo 1), tRNA^{Ser}_{GCU} (oligo 2); Blot C: tRNA^{Leu}_{CAA} (oligo 1), tRNA^{Pro} (oligo 2); Blot D: tRNA^{Lys} (oligo 1), tRNA^{Leu}_{UAG} (oligo 2); Blot E: tRNA^{Ser}_{CGA} (oligo 1), tRNA^{Tyr} (oligo 2). The probing order for Figure S9A was: Blot A: tRNA^{Trp} (oligo 1), tRNA^{Leu}_{CAA} (oligo 2); Blot B: tRNA^{Ser}_{GCU} (oligo 1), tRNA^{Ile} (oligo 2). tRNA^{Tyr} and fitRNA^{Leu}_{UAG} were not detected and therefore the data was not included.

To strip the oligonucleotide from the membrane, membranes were incubated with 15mL 0.1% SDS at 75°C for 10min with gentle shaking or rotation. This was repeated 5 more times. Membranes were rinsed with 15mL 5x saline-sodium citrate (SSC) buffer at 37°C for 5min before incubation with a second probe.

Western blot analysis

Protein was isolated by resuspending cell pellets obtained from mid-log phase cultures in 100µL lysis buffer (50mM Tris-HCl pH 7.4, 150mM NaCl, 25mM EDTA pH 8.0, 1% Triton X-100, 0.5% SDS, 1.5µL/mL protease inhibitor cocktail set IV (EMD Millipore), and 10mM PMSF). Acid-washed glass beads were added to the 1.5mL microcentrifuge tube at a 1:1 ratio. Lysate and beads were vortexed at max speed at 4°C for 5min. Tubes were placed on ice for 2min, then vortexed again. Tubes were centrifuged at 15000 rpm at 4°C for 5min. The supernatant was transferred to a new 1.5mL microcentrifuge tube and protein concentration was measured using the Bio-Rad Protein Assay Dye Reagent. For gel electrophoresis, 10µg of protein was combined with 4x loading dye, incubated at 95°C for 5min and loaded into the wells of a 4-12% Bis-Tris polyacrylamide gel. The protein was then transferred to a nitrocellulose membrane before incubation with the following primary and secondary antibodies. The primary antibodies used in this study were: mouse anti-6xHIS antibody (Invitrogen #MA1-21315, 1:1000), mouse anti-Nsp1 antibody (EnCor Biotech #MCA-32D6, 1:1000), rabbit anti-Gsp1 antibody (Abcam #ab4781, 1:1500), mouse anti-Nup1 (mAb 414, 1:1000, gift from LI Davis),⁶⁴ rabbit anti-Atp2 (1:1000, gift from M Yaffe; originally from the G. Schatz lab)⁶⁵ and rabbit anti-Rna1 (6142 at 10 weeks,⁶⁶ 1:10,000). The secondary antibodies used were goat anti-mouse IgG antibodies (IRDye® 680 RD, LI-COR, 1:1000) and goat anti-rabbit IgG antibodies (IRDye® 800 CW, LI-COR, 1:1,000). The IR signals were visualized by LICOR ODYSSEY platform machine and images were obtained and quantified using the LI-COR Image Studio™ software.

Yeast subcellular fractionation

Subcellular fractionation of yeast cells was based on the protocol in Neumann et al. (2023).⁷⁹ Briefly, 200mL yeast cultures were grown to mid-log phase (OD_{600} of 0.4–0.6), divided into four 50mL centrifuge tubes and centrifuged at 3000g for 5min at room temperature. Cells were transferred to 1.5mL microcentrifuge tubes (4 tubes total) and centrifuged at 10500rpm for 1.5min. Spheroplasts were generated by gently resuspending the cells in 1mL spheroplast buffer (1M sorbitol, 10mM EDTA pH 8.0) supplemented with 25U of Zymolyase and incubating at room temperature for approximately 45–60min until 50–60% of cells became spheroplasts. For DOX-treated cells, 10µg/mL DOX was added to the spheroplast buffer. Therefore, the time of DOX treatment for the fractionation experiments equals the time cell cultures were incubated with DOX plus the time cells were incubated in DOX-supplemented spheroplast buffer. The 4 tubes containing spheroplasts were centrifuged at 3100rpm at 4°C for 5min. The supernatant was removed and spheroplasts were gently resuspended in 250µL Ficoll buffer (10mM HEPES pH 6.0, 18% Ficoll 400). Spheroplasts from the 4 tubes were combined into 2 tubes of 500µL each. Spheroplasts were lysed by adding 600µL lysis buffer (10mM HEPES pH 6.0, 50mM NaCl, 1mM MgCl₂, 80U/mL RiboLock RNase inhibitor and 2µL/mL protease inhibitor cocktail set IV) to each tube and inverting several times to mix. 100µL of lysate was reserved and frozen at -80°C for use in downstream protein and RNA analysis. The remaining lysate was centrifuged at 4000rpm at 4°C for 15min. The supernatant, which contains the cytoplasmic fraction, was transferred to two new 1.5mL microcentrifuge tubes. The pellet, which contains organelles and intact cells, was kept on ice while the cytoplasmic fraction was processed. The tubes containing the cytoplasmic fraction were centrifuged at 3000rpm at 4°C for 5min. The supernatant was again transferred to new 1.5mL microcentrifuge tubes and frozen at -80°C. This is the cytoplasmic fraction. To obtain the organellar fraction, the pellets that were previously stored on ice were resuspended in 0.5mL NIB buffer (17% glycerol, 50mM MOPS pH 7.5, 150mM KAc, 2mM MgCl₂, 500µM spermidine, 150µM spermine and 16U/mL RiboLock RNase inhibitor) and combined into one tube. The tube was centrifuged at 3000rpm at 4°C for 1.5min to pellet any intact cells. The supernatant was transferred to a new 1.5mL tube and the previous centrifugation was repeated. The supernatant was transferred to a new tube and centrifuged at 15000rpm at 4°C for 5min. The supernatant was removed and the pellet, containing the organelles, was resuspended in 400µL NIB buffer and frozen at -80°C. This is the organellar fraction.

For RNA isolation, 400µL of LETS buffer (10mM Tris-HCl pH 7.5, 100mM LiCl, 10mM EDTA pH 8.0 and 0.2% SDS) was added to 1.5mL microcentrifuge tubes containing approximately 50µL of lysate, 400µL of cytoplasmic fraction or 400µL of organellar fraction. Phenol-chloroform extraction and isopropanol precipitation was performed as described above for total RNA isolation, except 300µL phenol and chloroform were added in the first extraction step and 200µL of each were added in the second step. For protein analysis, protein concentration measurements and western blotting were performed as described above.

QUANTIFICATION AND STATISTICAL ANALYSIS

All data are expressed as mean \pm SEM. N values indicate the number of biological replicates per experiment. Each experiment was performed at least in triplicate. The results from one representative experiment are shown. Statistical analyses were performed using the GraphPad Prism 9 software. Unpaired t-tests with a two-tailed P value were used when comparing two groups. One-way ANOVA with Sidak's multiple comparisons test was used when comparing more than two groups. Two-way ANOVA was used when comparing two independent variables. For Figures 2D and 2E, the Benjamini, Krieger, and Yekutieli method was used to control the false discovery rate and asterisks indicate $q < 0.05$. A p value of < 0.05 was considered significant. Statistical significance is denoted in all figures as: * $p < 0.05$, ** $p < 0.01$, *** $p < 0.001$, **** $p < 0.0001$, ns: $p > 0.05$, unless otherwise noted.